IS-T-312

SURFACE SUPERCONDUCTIVITY IN HIGH PURITY NIOBIUM

by

Jerome Edward Ostenson

A Thesis Submitted to the

Graduate Faculty in Partial Fulfillment of

The Requirements for the Degree of

MASTER OF SCIENCE

Major Subject: Solid State Physics

Approved:

D.K. Finnemore
In Charge of Major Work

D.J. Zaffarano
Head of Major Department

J.B. Page / E.M. Hatch
Dean of Graduate College

Iowa State University
Of Science and Technology
Ames, Iowa

May 1969

IS-T- 312

MASTER

AMES LABORATORY

Iowa State University

Ames, Iowa

AEC Contract No. W-7405-eng-82

SURFACE SUPERCONDUCTIVITY IN HIGH PURITY NIOBIUM

by

Jerome Edward Ostenson

M.S. Thesis, May 1969

TABLE OF CONTENTS

SURFACE SUPERCONDUCTIVITY IN HIGH PURITY NIOBIUM*

Jerome Edward Ostenson

Under the supervision of D. K. Finnemore
From the Department of Physics
Iowa State University of Science and Technology

ABSTRACT

At temperatures very close to the superconducting critical temperature, the nucleation field H_{c3} does not agree with the predictions of Saint James and de Gennes. As T approaches T_c, the ratio $C = H_{c3}/H_{c2}$ approaches 1.0 rather than the theoretical value of 1.7. Deviation from the theory have an exponential temperature dependence with a characteristic interval of about 0.133 K.

*USAEC REPORT IS-T-312. This work was performed under Contract W-7405-eng-82 with the Atomic Energy Commission.

INTRODUCTION

Since the discovery of superconductivity by Kammerlingh Onnes[1] in 1911 a great deal has been learned about the magnetic properties of superconducting materials. In 1933 Meissner and Ochsenfeld[2] found that very pure lead and tin would exhibit perfect diamagnetism, a condition in which the magnetic induction, B, is identically zero except for a layer about 400 Å thick at the surface. This surface layer carries the current required to insure that $B = 0$ inside. If the materials were rather impure, however, the perfect diamagnetism, or Meissner effect, shown by the solid line (Fig. 1) did not always occur but the magnetic behavior was substantially more complicated. As was first pointed out by Abrikosov[3] and by Goodman[4], there are really two distinct categories of superconductors which can be distinguished by the ratio of the penetration depth, λ, to the coherence distance, ξ. Metals with $\lambda/\xi < 1$ are called type I and show magnetization curves similar to the solid curve (Fig. 1). Metals with $\lambda/\xi > 1$ are called type II and show magnetization curves similar to the dashed curve (Fig. 1). For type II superconductors there are two distinct regions with different magnetic behavior. At low fields the sample shows $B = 0$ similar to a type I material but at a characteristic field, H_{c1}, magnetic flux begins to penetrate the sample in the form of quantized vortex lines and the average B is greater than zero. As the field increases the vortices become more numerous until at a higher characteristic field, H_{c2}, the sample appears to revert to a completely normal state.

Samples often showed traces of superconductivity above H_{c2}, and for many years this effect was attributed to a lack of homogeneity in the samples. In 1963, however Saint James and de Gennes[5] showed that one

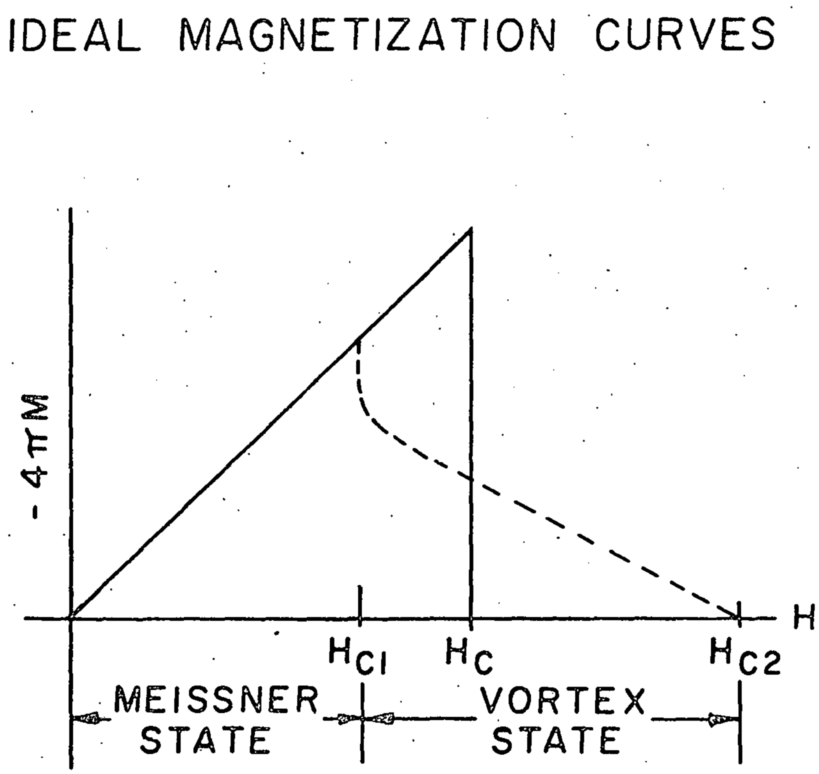

Fig. 1. Ideal magnetization curves for type I and type II superconductors

might expect a sheath of superconductivity on the surface of a sample up to a field of 1.7 H_{c2}. A number of experiments immediately confirmed the existence of this sheath[6], and, in fact, the value 1.695 H_{c2} is very close to many of the experimental results. For type II superconductors there are at least three distinct regions, the Meissner region ($H < H_{c1}$), the vortex region ($H_{c1} < H < H_{c2}$), and the sheath region ($H_{c2} < H < H_{c3}$). Most pure materials exhibit type I ($\lambda/\xi < 1$) behavior unless impurities are added to make them type II. It has been shown, however, that niobium is one of the few pure metals that is intrinsicaly type II[7]. For the case of Nb, the Fermi velocity, v_F, is very small and the transition temperature is very high. Hence $\xi_o = 0.18\ \hbar v_F/kT_c$ is unusually small.

In connection with a study of the bulk superconducting properties of niobium an attempt was made to look for the superconducting sheath at fields greater than H_{c2}[7]. This surface superconducting state had been studied by resistive measurements as well as by mutual inductance measurements, but there remained a large number of unanswered questions. In the resistive measurements the results were strongly dependent on the current through the sample. The results of the mutual inductance measurements seemed to indicate the presence of H_{c3} at 4.2 K, but not at 8.0 K. Difficulties in obtaining reproducible data precluded further studies of the problem at that time. Hence, further work seemed to be in order. This study of H_{c3} in high purity niobium was begun with special emphasis being placed on getting good data near T_c and determining if, in fact, H_{c3} did disappear, at what temperature this took place.

Several theoretical improvements on the original Saint James-de Gennes model have recently been published. Calculations by Ebneth and Tewordt[8] on the effect that impurities have on the ratio $C = H_{c3}/H_{c2}$ near T_c predicted that in the clean limit

$$C = 1.695 + 1.04\,\epsilon \qquad (1)$$

where $\epsilon = (T_c - T)/T_c$. More recent calculations by Lüders[9] give

$$C = 1.695(1 + p\,\frac{44}{224}\frac{\zeta(4)}{\zeta(3)}\,B\,\varepsilon_o^{-1/2}\,\tau^{-1/2} \qquad (2)$$

where:

$$\tau = \frac{12}{7\zeta(3)}\,\epsilon$$

$$\varepsilon_o = 1.695^{-1}$$

$$B = 1.36$$

and p is a parameter $(0 < p < 1)$ describing the reflective diffusivity of the surface. $p = 1$ approximates the actual physical situation of high diffusivity whereas $p = 0$ corresponds to the case of perfect specular reflection. Recent experiments by Webb[10] on high purity niobium agree generally with the form put forth by Ebneth and Tewordt, but the data are not sufficiently precise to clearly distinguish between the two theories. He finds that his data above $t = 0.85$ fits the expression

$$C = 1.67\,^{+0.05}_{-0.02} + 0.8\,\epsilon \qquad (3)$$

In considering the measurements that have been made one also notices that most of the data ends as $\epsilon \rightarrow 0.025$ and that in this region near T_c the scatter is generally worse than at lower temperatures. Early qualitative measurements made on a number of different samples of niobium in this laboratory gave us the impression that C did not come in to a value of about 1.7 at T_c, as measurements by others had indicated. Instead it seemed to round off and go toward 1.0 at T_c. The measurements to be presented here will be considering especially a set of data in the region $0.0028 \leq \epsilon \leq 0.086$, where twelve of the eighteen runs were for $\epsilon \leq 0.0253$. We will, in fact, show that C departs from the predicted value of 1.7 and drops sharply toward 1.0 at T_c. The difference

$$\delta h = 1.7 - C(\epsilon) \qquad (4)$$

can be fit very nicely to an expression of the form

$$\delta h \doteq \alpha\, e^{\beta\sqrt{\epsilon}} . \qquad (5)$$

SAMPLE PREPARATION

The niobium used in this experiment was obtained originally from the DuPont Corporation in shot form identified as Lot No. DH-715. Analysis of this material indicated the tantalum content to be less than 25 ppm. This shot was arc melted and swaged into a 0.100 inch rod for electro-transport purification as sample JN-56. During the electro-transport treatment the sample was heated to a temperature of 1800 C by passing a d-c current through it in a vacuum of $5\text{-}8 \times 10^{-9}$ torr for 100 hours. After this treatment the sample had a resistivity ratio of 1023*. For the measurements described here the sample was swaged further, down to 0.025 inches in diameter.

A three inch segment of this wire was spot welded onto a 0.060 inch tungsten support rod for further degassing (Fig. 2). Around the sample was spiraled a filament of 0.010 inch tantalum wire with a pitch of about two turns per inch. After sealing the sample and filament assembly into the stainless steel high vacuum system, the system was pumped to a pressure of less than 10^{-7} torr with an Ultek ion pump and the filaments were outgassed by passing a 5.5 ampere current through them. As the filaments outgassed the pressure dropped to 1.5×10^{-8} torr with the power on and when the power was removed from the filaments the pressure fell to 7.4×10^{-9} torr. The entire vacuum system was then baked at 250 C with an oven and heating tape, with the pressure remaining below 8×10^{-8} torr at all times. After heating and complete cooldown the final pressure in the chamber was 9.6×10^{-10} torr.

---

*Schmidt, F. R., Ames Lab A.E.C., Ames, Iowa. Sample history data. Private communication. 1968.

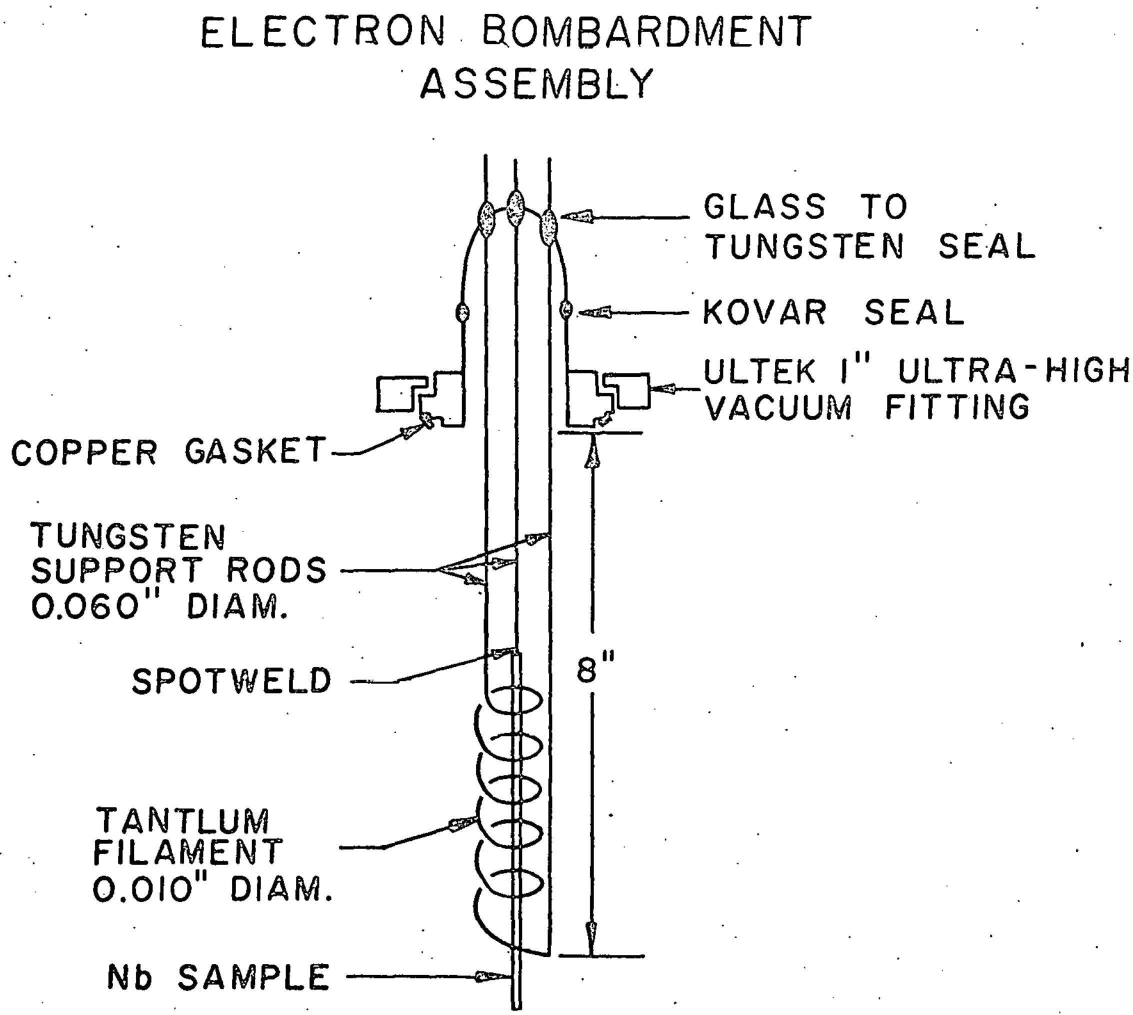

Fig. 2. The sample support assembly for the high vacuum degassing system.

The samples were then ready to be outgassed. By applying a high voltage to the sample and passing a current through the filament around the sample, we have in effect a simple diode type vacuum tube, and the sample is heated by electron bombardment. Sample OJ-4-85 was heated in a vacuum better than 9×10^{-9} torr with the power level being increased gradually to 100 watts over a five hour time interval. The pressure in the chamber when the power reached 100 watts was 8.2×10^{-9} torr but fell to a final pressure of 2.4×10^{-9} torr as this power level was held for eighteen hours. After this period the power level was slowly raised to 110 watts where the lower centimeter of the sample melted and fell off. At no time during the heating of the sample was the current in the filament raised to the level used to outgas the filament. Upon completion of the sample treatment all heating power was cut off and the sample cooled to below red heat in less than twenty seconds.

Sample OJ-4-86 was given a similar treatment. Initial attempts to bring up the power level were frustrated by arcing between the sample support and the filament supports. A number of fuses were blown before the arcing stopped and the heating was continued. With the sample power at 80 watts and the pressure at 2.6×10^{-9} torr the power was raised to 101 watts over a four hour period and held for twenty hours at which time the pressure was at 2.9×10^{-9} torr. The power was then raised to 109 watts and held for an additional seven hours with the pressure less than 3×10^{-9} torr. During this period the lower end of the sample slowly melted into a ball at the bottom of the sample and remained there as the sample was slowly cooled over an eighteen hour period with the pressure dropping to a final pressure of 9.7×10^{-11} torr.

The samples remained in the high vacuum chamber until they were removed to be placed in the susceptibility cryostat. At that time the sample was cut from the support with a pair of side cutters, and the end farthest from the support was severed from the rest of the sample with a new razor blade using a piece of clean aluminum as a backing plate. Samples prepared in this manner were only exposed to the atmosphere for a period of about ten to fifteen minutes before being sealed in the cryostat with a vacuum or helium gas environment. Subsequent to the susceptibility measurements the resistivity ratio was remeasured and found to be at least 800.

EXPERIMENTAL SYSTEMS

The dewar system (Fig. 3) used in this experiment is a standard design for work in a magnetic field at temperatures from 1 to 20 K[11]. The helium dewar which was made of brass and 321 stainless steel has a capacity of about four liters of liquid when the heat leak chamber is in place. Surrounding the tail of the dewar is a sixth order solenoid capable of producing 150.9 Oersteds per ampere. This solenoid is powered by a Spectromagnetic current regulated power supply which can deliver 50 amperes in a one ohm load with stability of $\pm 10^{-5}$ over an eight hour period. The current in the solenoid is determined by the voltage drop across a Rubicon 0.01 ohm, 100 ampere shunt using a Keithley Instruments Model 662 guarded differential voltmeter.

Cancellation of the horizontal and vertical components of the earth's field in the sample region of the cryostat is made, in the absence of any applied field, by a pair of Helmholtz coils. The currents required to cancel the earth's field were determined using a Bell "120" gaussmeter which had a full scale reading of 0.1 gauss. A Power Designs Model 5005R regulated power supply powered the Helmholtz coils through a current divider (Fig. 4) which determined the fraction of the current which passed through each coil.

Temperature control in the sample region was accomplished by pumping on the helium bath through a manostat (Fig. 5) for temperatures below 4.2 K. Before pumping the bath for temperatures below 4.2 K the vacuum space in the heat leak chamber as well as the heat leak chamber itself were subjected to an over pressure of helium gas in order to condense liquid helium around the sample. During the pumping operation these regions were

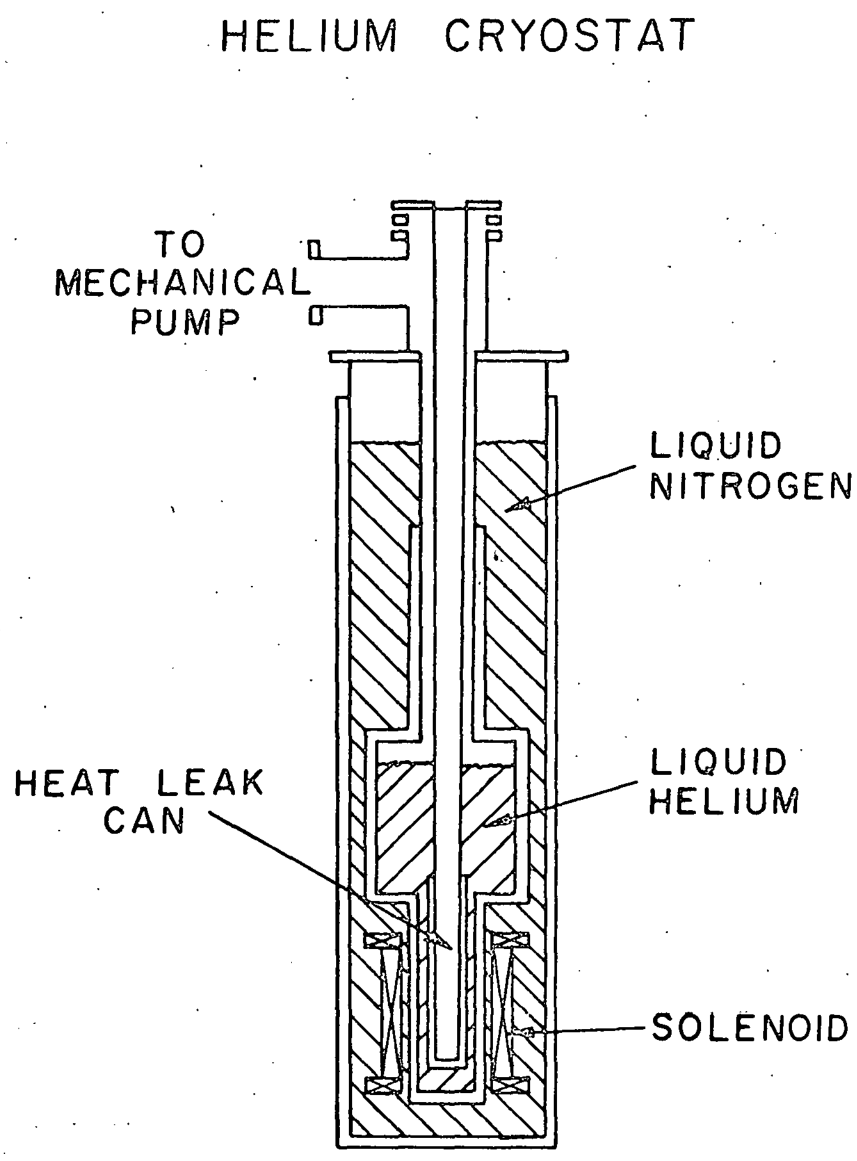

Fig. 3. A view of the cryogenic system used in this experiment

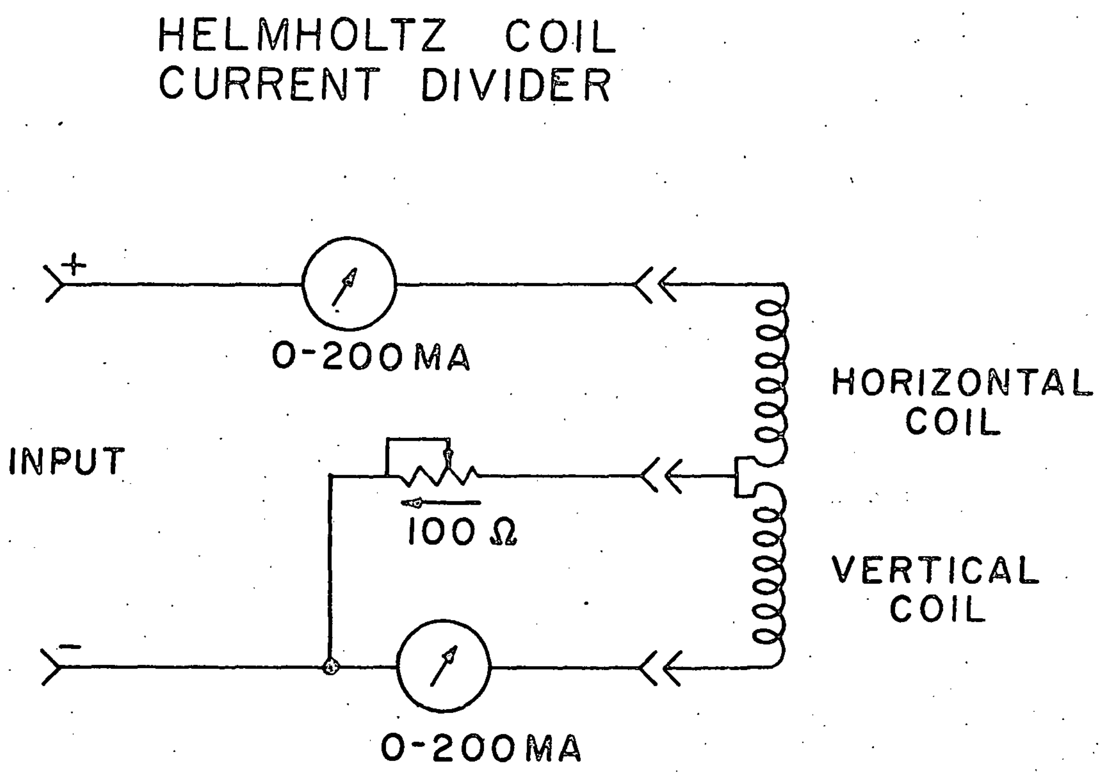

Fig. 4. The circuit used to adjust the current through the Helmholtz coils

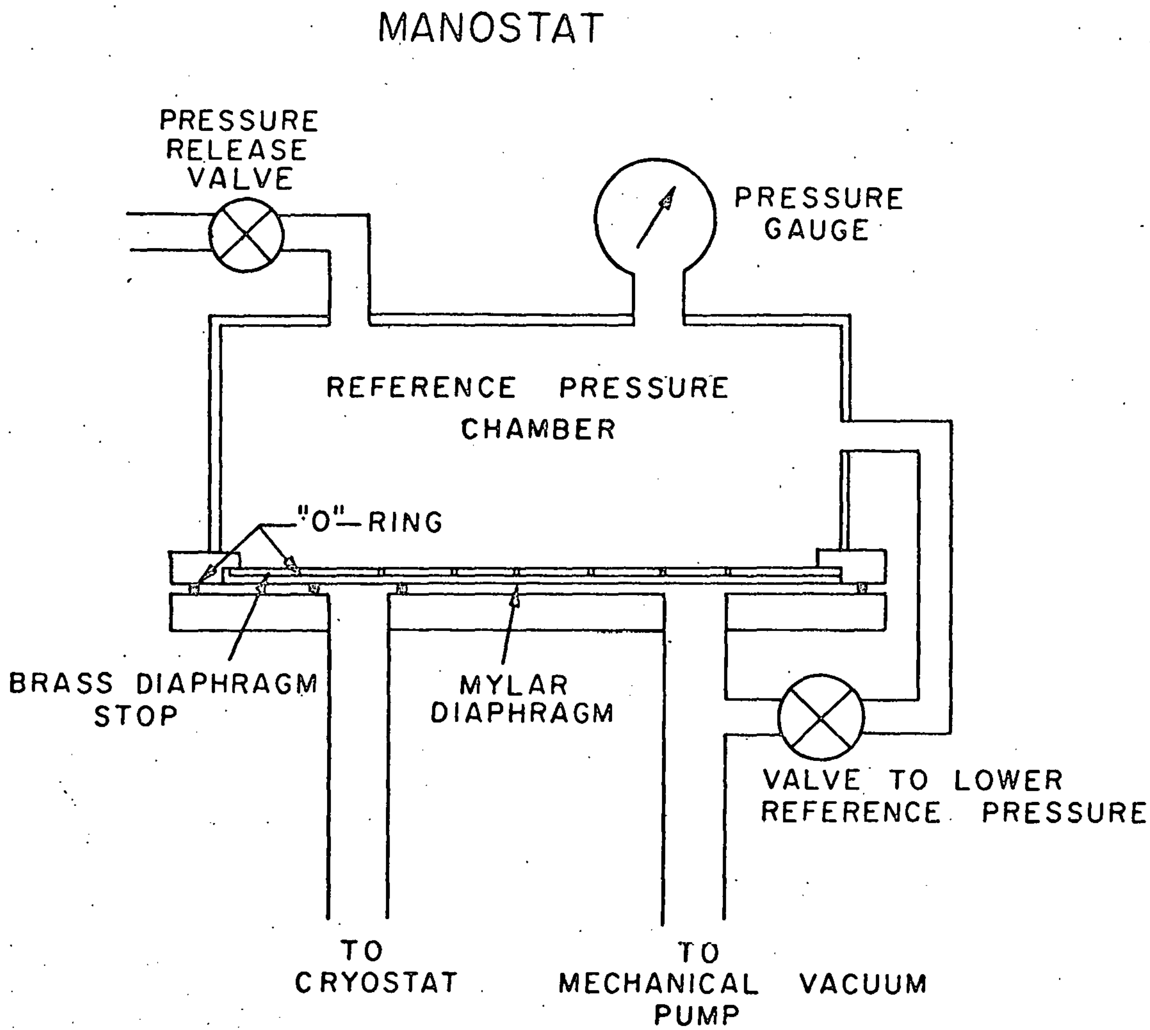

Fig. 5. A schematic of the pressure control manostat used to obtain temperatures below 4.2 K

kept at the same pressure as the surrounding bath using external connections.

When temperatures greater than 4.2 K were desired the heat leak chamber vacuum space was evacuated to a pressure of less than 10^{-3} torr and the sample chamber sealed at a pressure of less than 0.5 torr. A manganin heater astatically wound around the outside of the inner portion of the heat leak chamber, was used to elevate the temperature. On the bottom of this same portion of the heat leak chamber was mounted an ordinary radio resistor to be used as the temperature control element. The resistance of this element was monitored with a Wheatstone bridge (Fig. 6) with the off balance of the bridge being fed into a Hewlett-Packard Model 419A d-c null voltmeter which amplified the signal so that it could be displayed on a 10 millivolt chart recorder for a continuous record of the temperature. On the recorder was mounted a cam and microswitch combination which was used as an increment switch to adjust the heater (Fig. 7) power at a given set point on the recorder.

The sample coils (Fig. 8) were designed so that the entire system would be symmetric about the sample. When the sample was in the center of the applied field it was also centered in the large center portion of the measuring coils. No special attempt was made to make the measuring coils exactly astatic, but the end sections of the secondary were wound with 2% more turns to partially compensate for the drop off of the measuring field due to the finite length of the primary coil which was wound directly beneath the secondary coils. Background runs were made at various temperatures to determine if there were any contributions to the data due to changing susceptibility in any of the materials in the area of the measuring fields. At any given temperature where the background was measured the

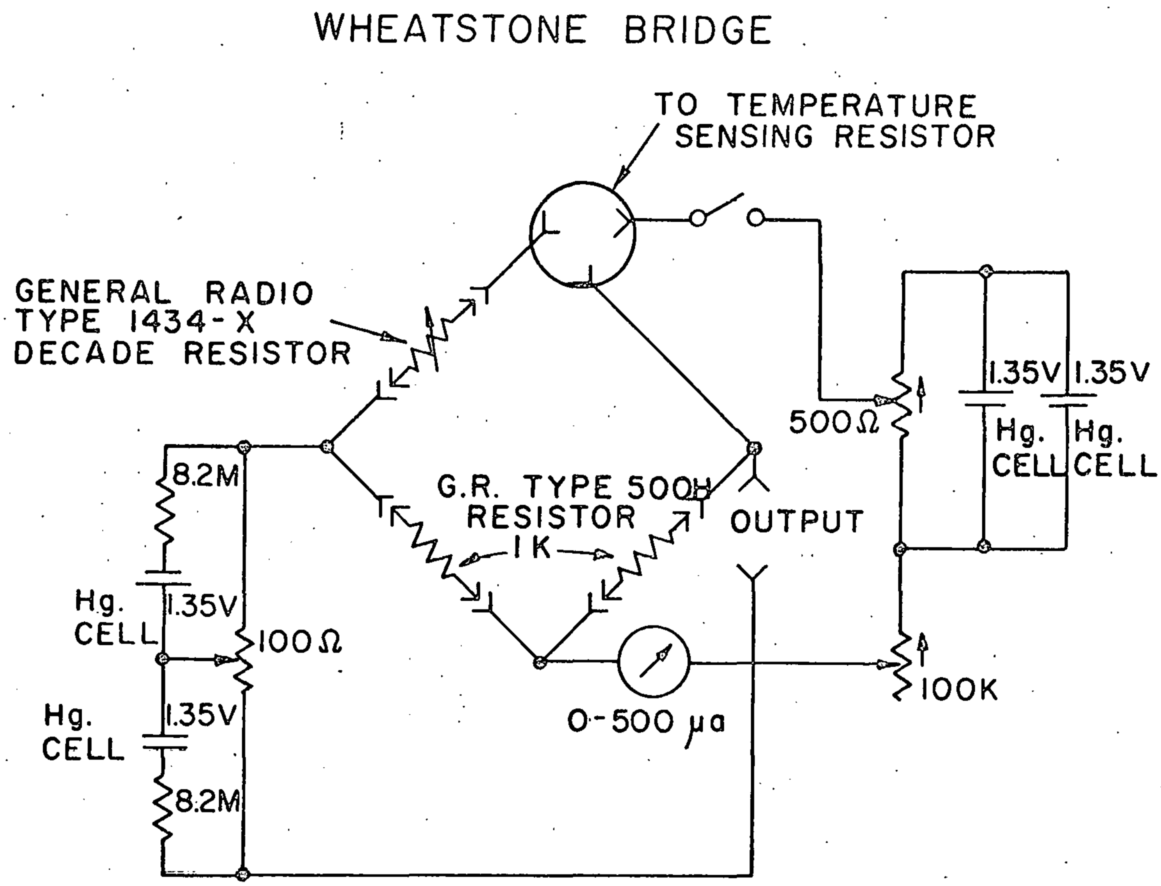

Fig. 6. Circuit diagram of the compensated Wheatstone bridge used for temperature control

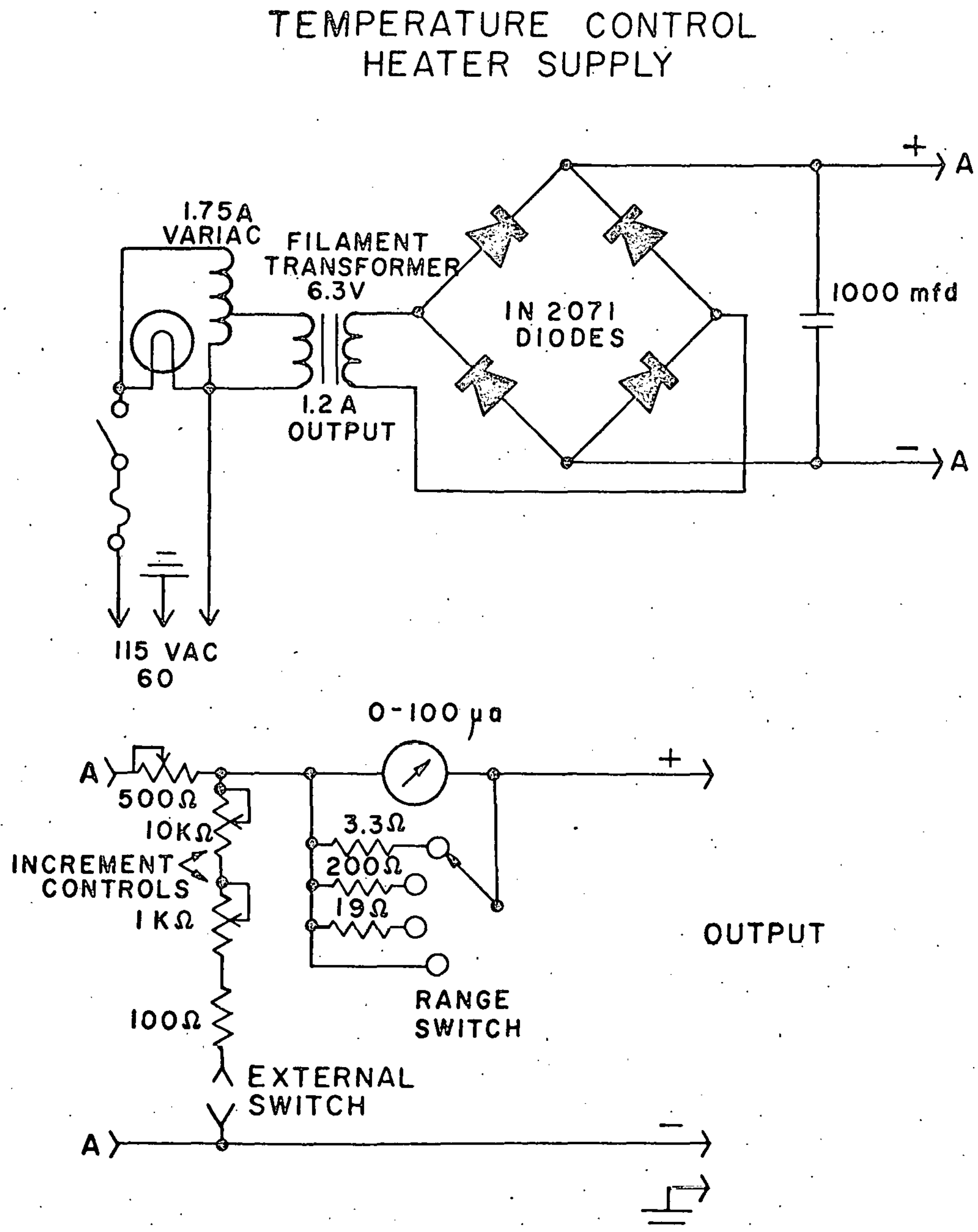

Fig. 7. The temperature control heater supply circuit

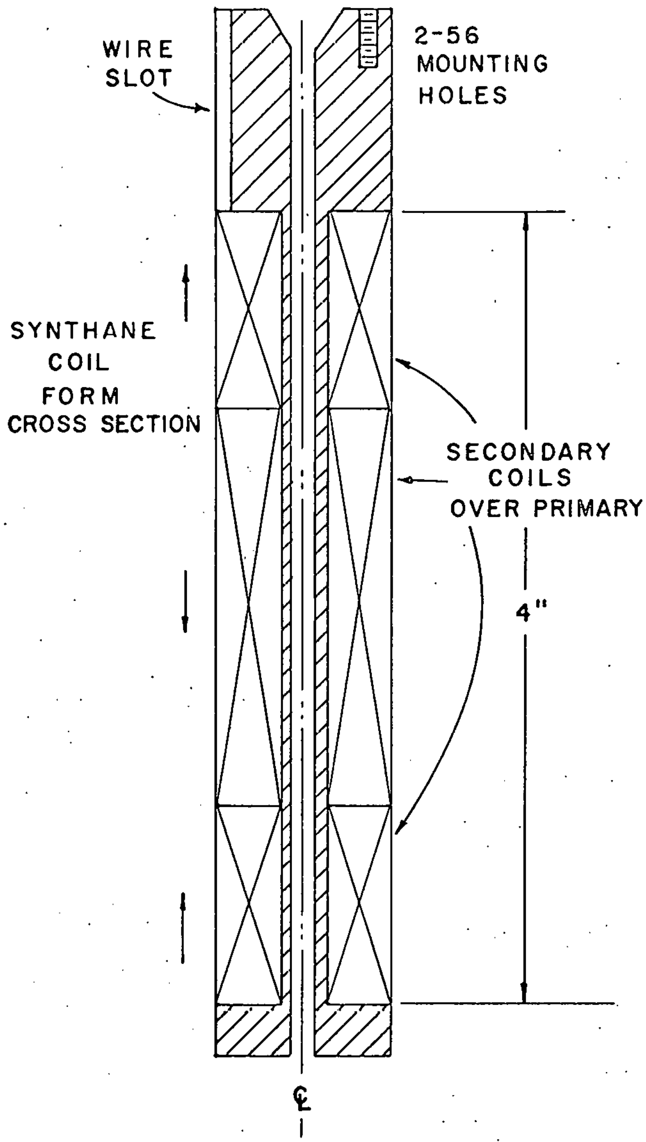

Fig. 8. The sample coils

total change in the readings was never more than 0.25% of the total change in the readings with a sample present going from completely normal to completely superconducting.

With a sample in place the output voltages of the measuring coils were on the order of 500 μv p-p inductive and 20 μv p-p in phase resistive. A complete transition in the sample would cause a net change in the inductive voltage of about 15 μv p-p and a change of 5 μv p-p in the resistive voltage. Changes in the output of the measuring coils due to the sample transition were measured using a mutual induction comparison bridge (Fig. 9). This bridge balances the output of the measuring coils against a fixed mutual inductance at room temperature using a ratio transformer to divide the output of the fixed "lump" to exactly balance the inductive component of the signal from the measuring coils. This only balanced the inductive component so we must also introduce an in-phase voltage to balance the voltages due to eddy current losses and non-ideal inductors in the circuit. This voltage is generated across a one ohm resistor placed in the detection portion of the bridge which is driven by a resistive network directly from the primary loop on the oscillator. The read out on the resistive network is such that the voltage introduced into the detection circuit is proportional to 1/(11110000-R) where R is the dial read out.

A narrow band amplifier[12] is used to amplify the bridge output so that it may be observed on an oscilloscope which is used as a phase sensitive detector to insure that both components of the susceptibility are balanced out. The off balance display on the scope was an inclined ellipse which could be rotated by adjusting the ratio transformer while the size of the minor axis was affected by adjusting the resistive network. When

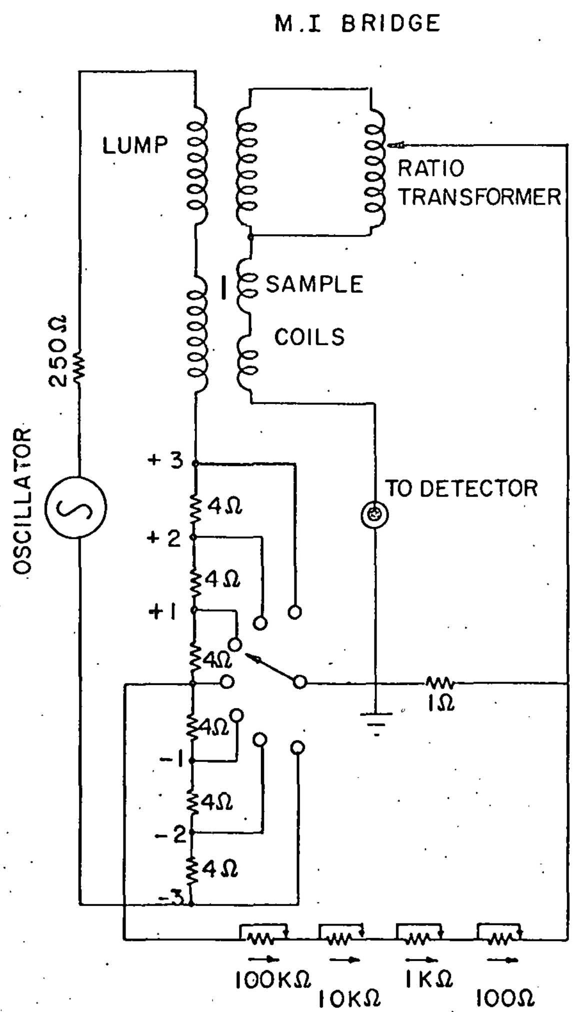

Fig. 9. The circuit diagram of the mutual inductance comparison bridge

the system was properly tuned the adjustments were nearly independent of each other.

A long copper rod was used as a sample holder (Fig. 10) to position the sample in the measuring coils. At the top end of the holder outside the measuring coils a germanium resistance thermometer was inserted into a close fitting hold with some Apiezon "N" grease to give some thermal contact to the sample holder. The leads from the thermometer were wrapped around the holder and held in place with GE No. 7031 insulating varnish to provide thermal contact between the leads and the holder. This is important since the primary heat path to the germanium element is through the leads. In these measurements where most of the data is near 9 K there should also be a reasonably good heat path through the case and the exchange gas surrounding the germanium element. The thermometer used in these measurements was the same thermometer as was used to measure the bulk superconducting properties of niobium[12]

In the preliminary runs there was quite a bit of scatter in the value of T_c as determined by the extrapolation of the H_{c3} data to $H_{c3} = 0$. It was determined that this scatter was primarily a thermometry problem due to varying amounts of exchange gas around the sample holder. By measuring H_{c3} at a given temperature according to the thermometer but varying the amount of exchange gas it was determined that if the pressure was kept below 0.5 torr in the sample space the scatter became less than .004 K. At these lower pressures there are no difficulties with convection currents.

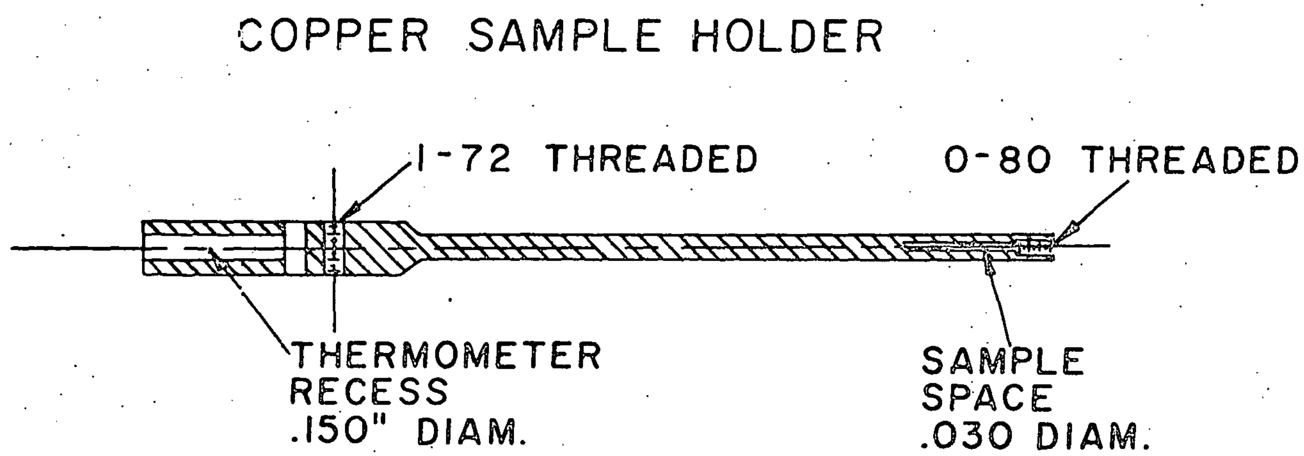

Fig. 10. The sample and thermometer holder assembly

EXPERIMENTAL TECHNIQUE

H_{c1}, H_{c2} and H_{c3} were determined from isothermal a-c susceptibility measurements from zero field to a field significantly above H_{c3} to insure being able to identify the breakover point at H_{c3}. At each field setting the inductance comparison bridge was balanced for both the inductive and resistive components, χ' and χ'' respectively. For temperatures below about 0.9 T_c the bridge could be balanced with a sensitivity of better than 0.2% of the total change from the completely superconducting to the completely normal state. As the temperature was raised nearer to T_c the output of the oscillator had to be reduced to a level which would guarantee that χ' was essentially constant over a full sweep of the measuring field. The extreme case was at the highest temperature measured where the measuring field was about 1.3% of H_{c3}. Various runs at different power levels showed the same breaks in the χ' vs. H plots as long as the breaks were well defined. If the power was too high the χ' structure completely disappeared, becoming a smooth curve. At temperatures above 8.8 K the oscillator output voltage was approximately 1% of that used at lower temperatures and as a result the sensitivity dropped to the point where a change of 1% of the superconducting to normal change could be detected.

Results from the bulk magnetization measurements[11] were used to determine the characteristic points on the χ' curves to be associated with H_{c1} and H_{c2}. H_{c1}, the first critical field, was identified as the minimum of the first dip on the χ' curve (Fig. 11). This dip dropped from ten to forty percent of a completely superconducting value. H_{c2} was identified as the sharp spike about midway between the completely normal and the completely superconducting values of χ'. The width of this spike was generally less

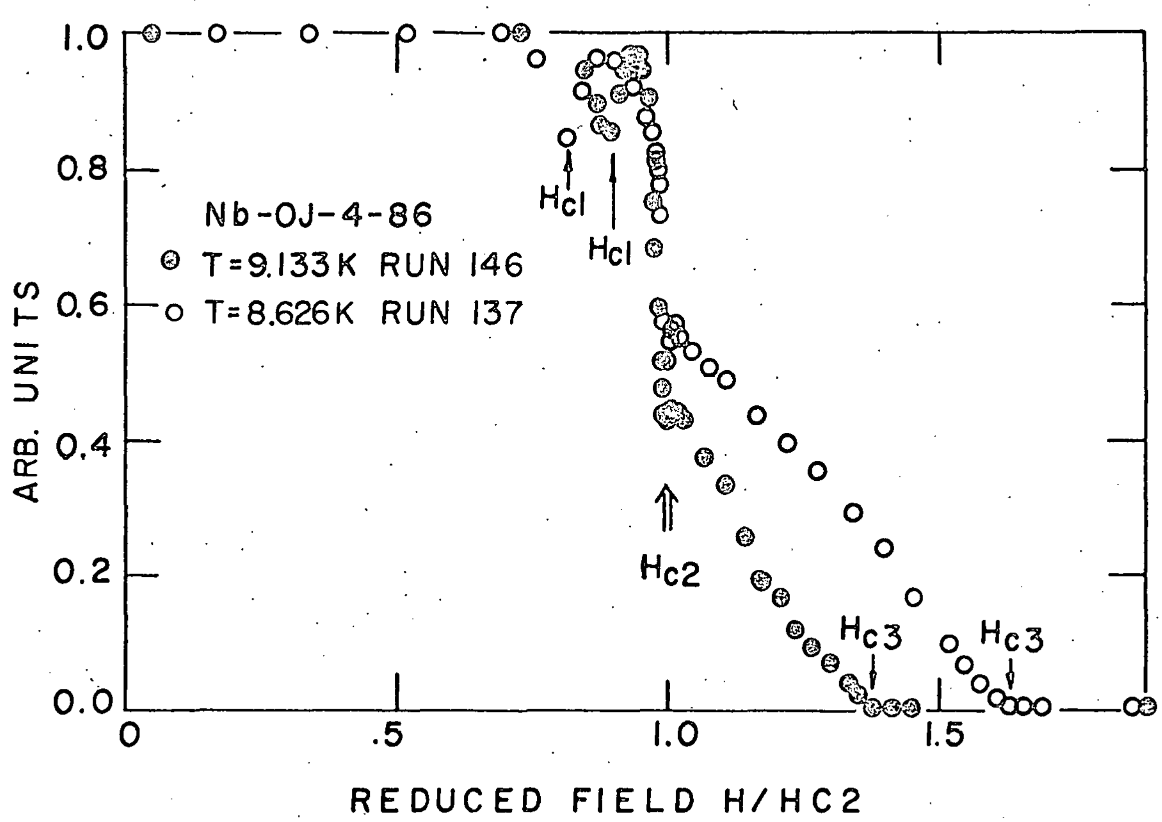

Fig. 11. A plot of χ' vs reduced field for two separate runs

than 2% of the applied field at this point on the curve. With these definitions of H_{c1} and H_{c2} there is agreement between the bulk magnetization measurements and the a-c susceptibility values over the entire temperature range. For comparison we plot the ratio H_{c1}/H_{c2} for both methods (Fig. 12) and note that at temperatures below 0.9 T_c the agreement is better than 1%, however above this point the bulk data drops off until at T_c it lies below the susceptibility measurements by 6%. It should be noted that in this region the scatter in the bulk data is on the order of 4% but the drop off is still easily observable. In this temperature range, the determination of H_{c1} from bulk data is difficult and the 6% shift is within the error of the bulk data. This very good agreement between the different methods of identifying H_{c1} and H_{c2} gives us confidence that these characteristic points on the χ' curve are correctly interpreted.

As the field is increased above H_{c2} the χ' readings continue to decrease but at a slower rate than in the region just below H_{c2}. Between H_{c2} and H_{c3}, χ' is linear to about 2% until H_{c3} where it becomes constant to 1% for nearly all the runs. H_{c3} is defined by the extrapolation of χ' above and below the break or that value where χ' becomes constant. If the results differed, both values were used. The lower temperature runs were the only runs to exhibit more than 1% change in χ' above H_{c3} where, at these temperatures, there seemed to be a slight slope in χ', but this was always so much less than the slope between H_{c2} and H_{c3} that the location of H_{c3} was still reasonably well defined. The breakover in χ' at H_{c3} became slightly rounded as the power was cut to enable us to take data very near to T_c.

As one looks at the phase diagram of a superconductor (Fig. 13) it is easily seen that the curves could be generated by changing the temperature

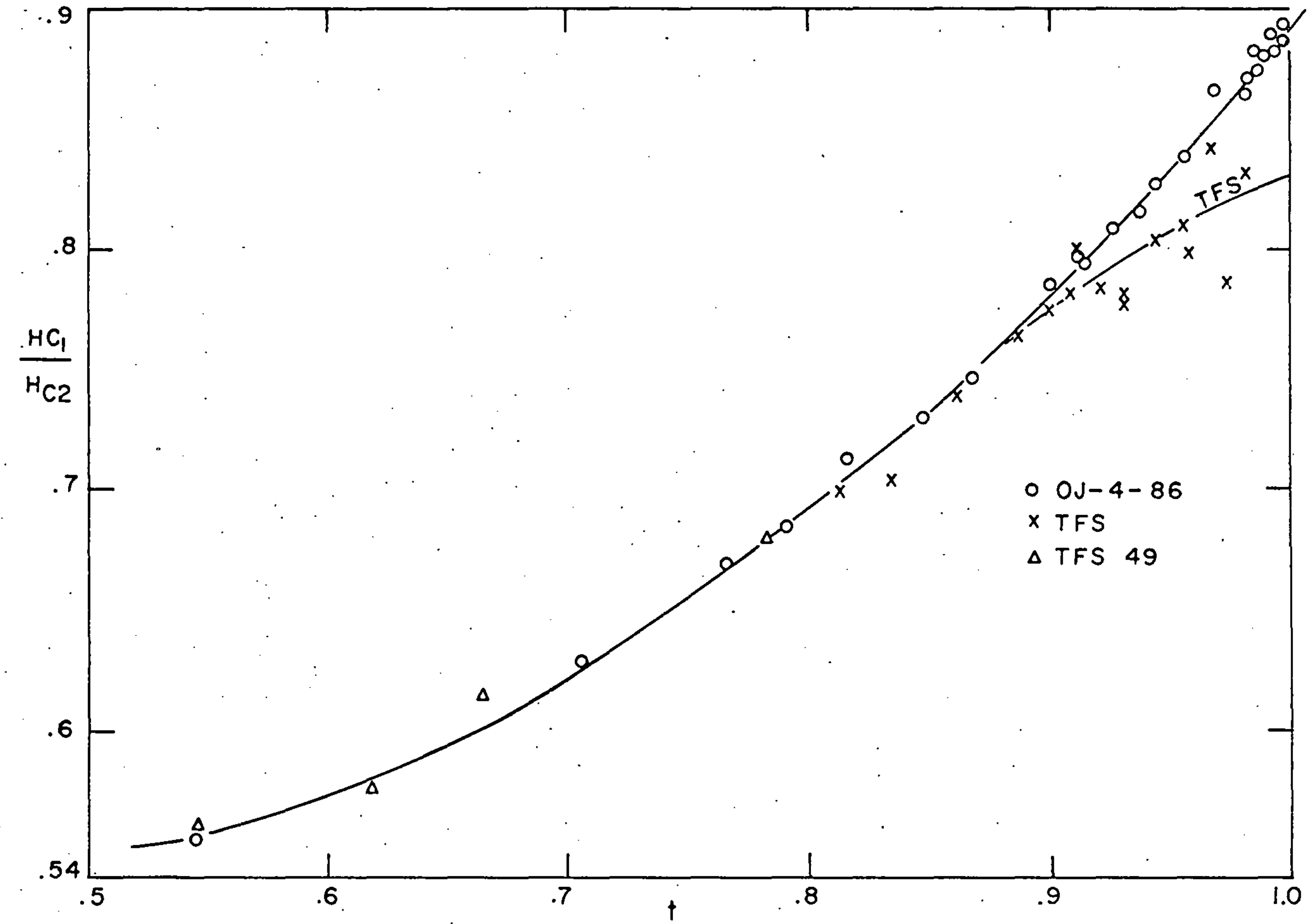

Fig. 12. A plot comparing the a-c susceptibility and bulk magnetization determinations of H_{c1}/H_{c2}

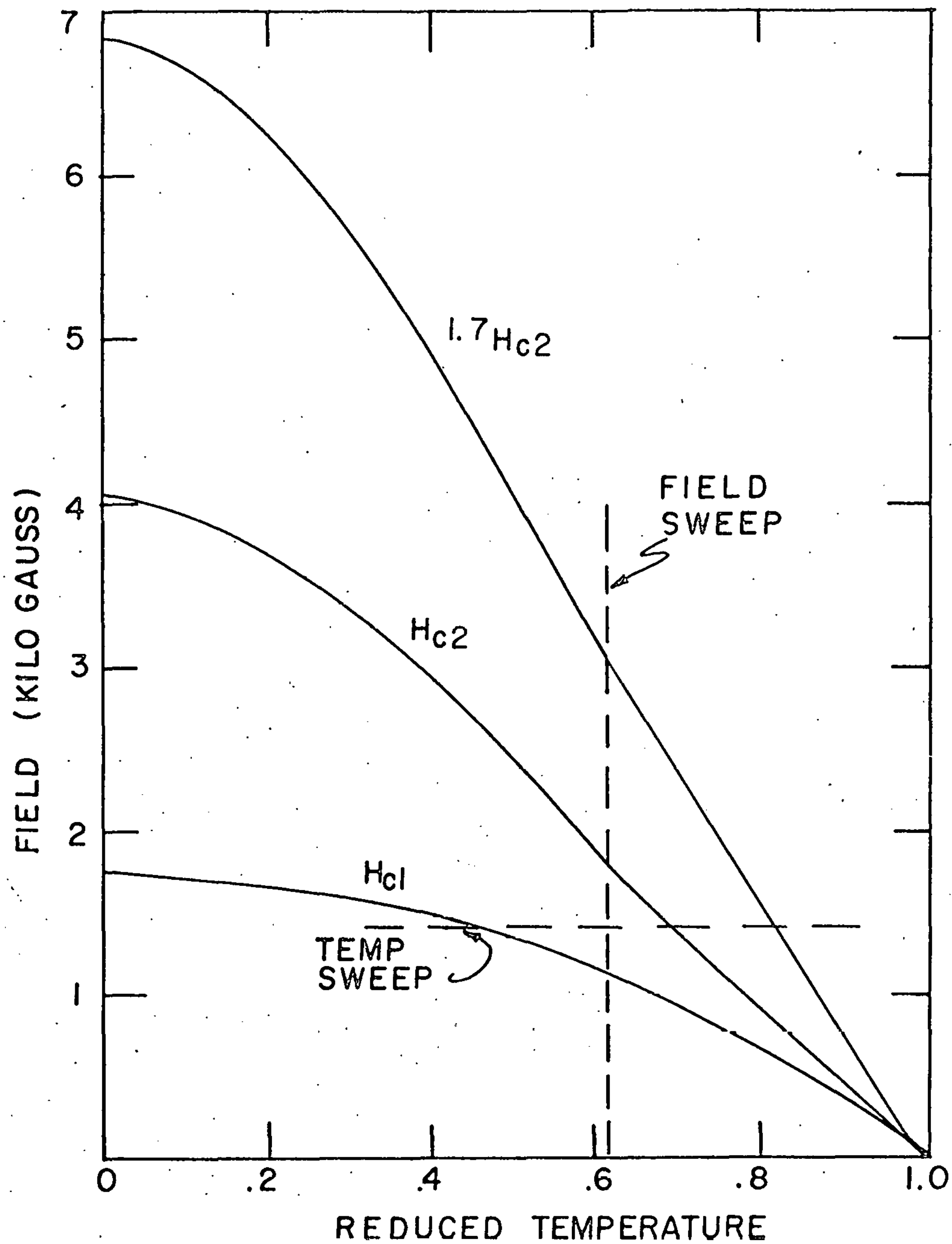

Fig. 13. A critical field curve for niobium from bulk magnetization data

and holding the field constant as well as changing the field while keeping the temperature constant. A few early runs were made at constant field before all the various temperature control problems were solved. Qualitatively these curves were similar to isothermal curves and could be evaluated in a similar manner. Unfortunately temperature control was poor and, the results for the various critical fields were off by about 10%. This is not unreasonable considering the condition of the systems at the time. No further runs of this type were made because the isothermal measurements were much easier to obtain experimentally.

Plots of χ'' as a function of field also show characteristic breaks at almost the same location as the breaks in the χ' curves. Data from some of the preliminary runs showed that the break at H_{c2} always occurred at a slightly lower field on the χ'' plot than on the χ' plot with the difference never being more than 5%. In the case of H_{c1} and H_{c3} however there was no definite pattern of this type. Differences of less than 2% were observed in the location of H_{c1} between the χ' and χ'' plots. For H_{c3}, there was some uncertainty in the definition of H_{c3} so the differences were larger and on the order of 8% between the different curves. In all of the following discussion all of the critical fields will be those determined from the χ' vs. H curves.

RESULTS AND DISCUSSION

Plots of χ' vs. H (Figs. 14-17) at different temperatures show essentially the same shape so it is convenient to consider the data in terms of the reduced variables H/H_{c2} and $t = T/T_c$. As the temperature is increased toward T_c the ratio H_{c1}/H_{c2} increases monotonically from 0.550 at 4.2 K to 0.892 at T_c in agreement with bulk measurements (Fig. 12).

C has the same shape as predicted by Hu and Korenman (H K)[13] for temperatures less than t = 0.9 but lies about 6% below the predicted value. Above this temperature the theory does not drop nearly as fast as the data. The H K expression

$$C = 1.695(1+0.614\epsilon - 0.577\epsilon^{3/2}) \qquad (6)$$

approaches 1.695 as T goes to T_c but the data appear to approach 1.0 as T goes to T_c. H K was expected to be valid in the region $0.1 \gtrsim \epsilon > 0.0$ but this is certainly not the case.

Several precautions have been taken to establish that these results are true equilibrium measurements of H_{c2} and H_{c3}. As was mentioned earlier there is a definite washing out of the information in the signal if the measuring field is too large. Measurements made subsequent to these presented here using more sensitive techniques indicate that the power level can be reduced by a factor of 100 with no change in H_{c3} or H_{c2}. The measurements presented here were repeated one month later on the same sample and the results were essentially the same. There was about a 5% reduction of C at all temperatures but the shape of the curve was unchanged. Another sample which was prepared in a similar manner over five years ago from a different lot of pure niobium shows essentially the same behavior as Nb-OJ-4-86 except that T_c was 0.050 K lower, and the values of C were a

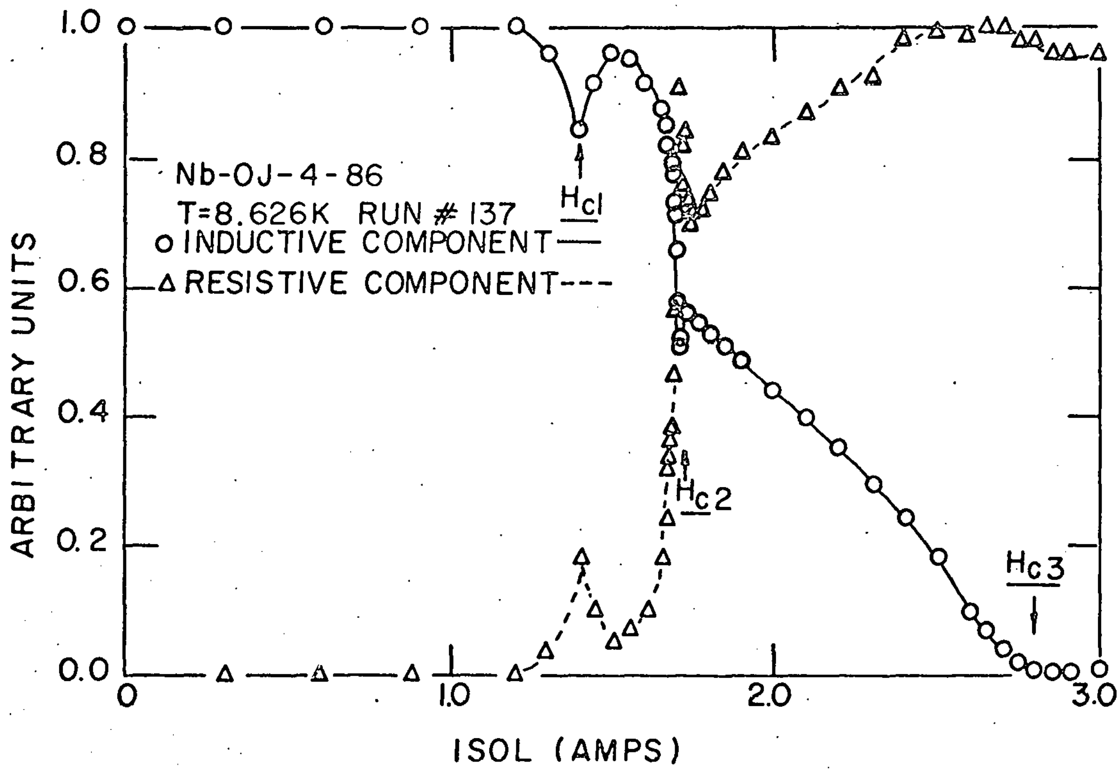

Fig. 14. The real and imaginary susceptibility of niobium at 8.626K

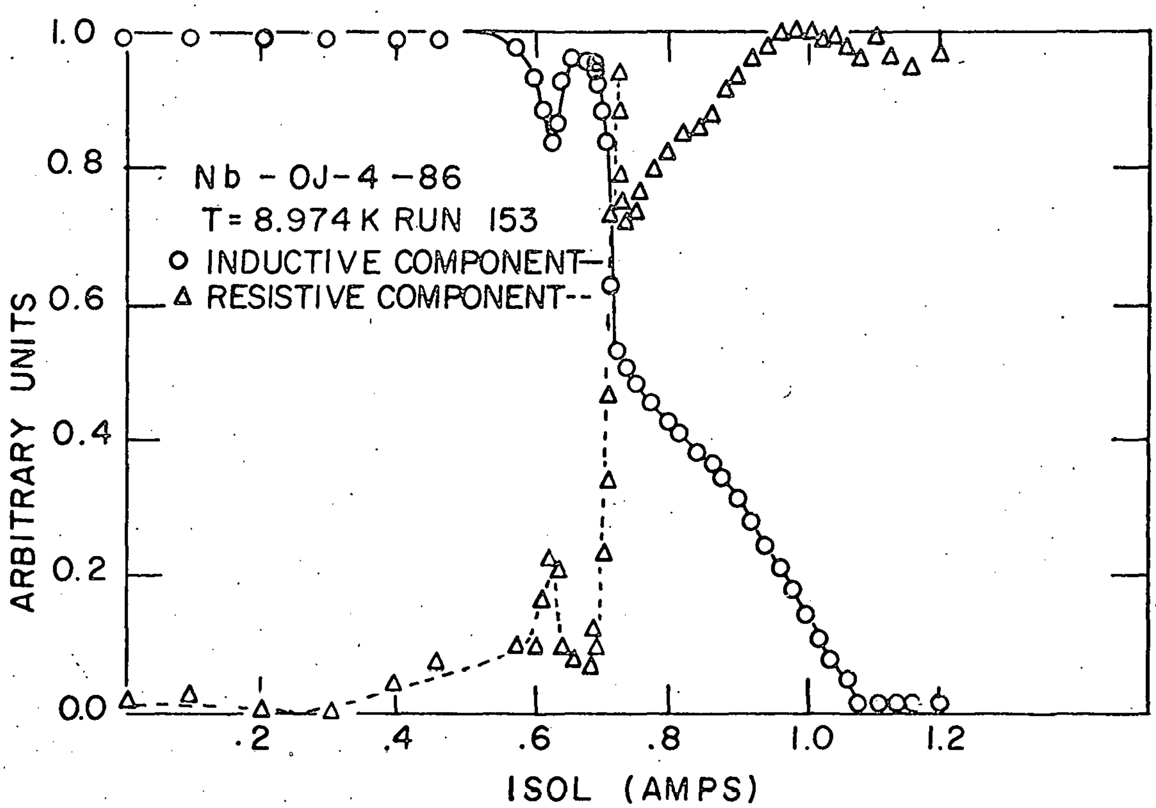

Fig. 15. The real and imaginary susceptibility of niobium at 8.974K

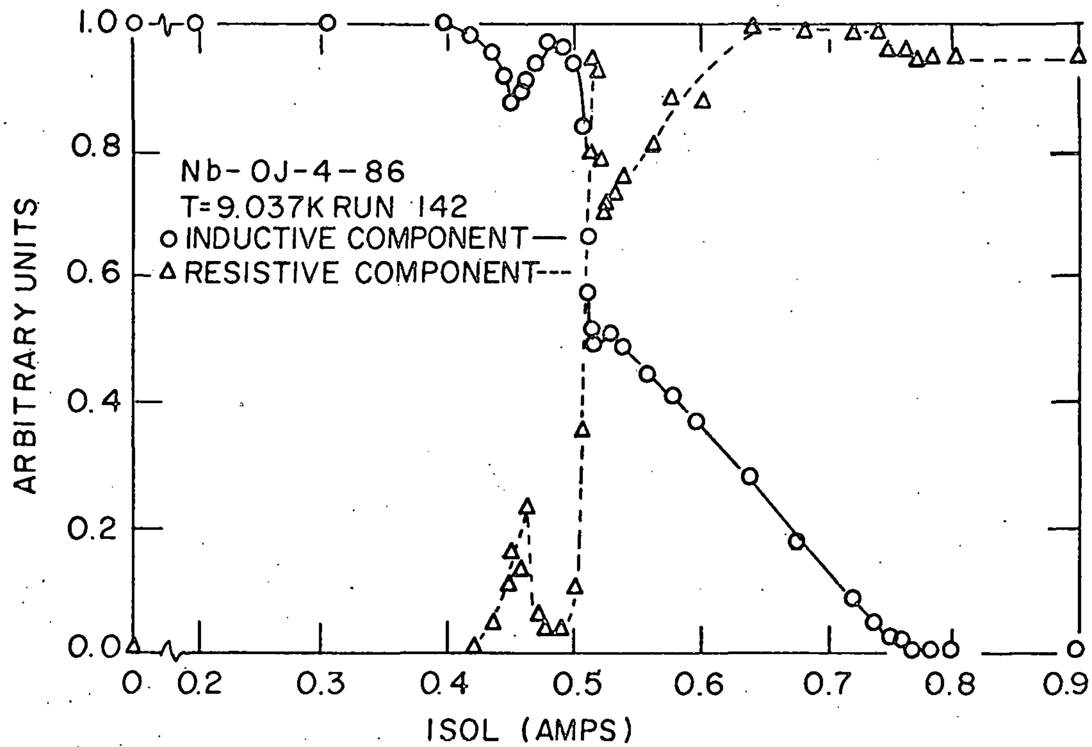

Fig. 16. The real and imaginary susceptibility of niobium at 9.037K

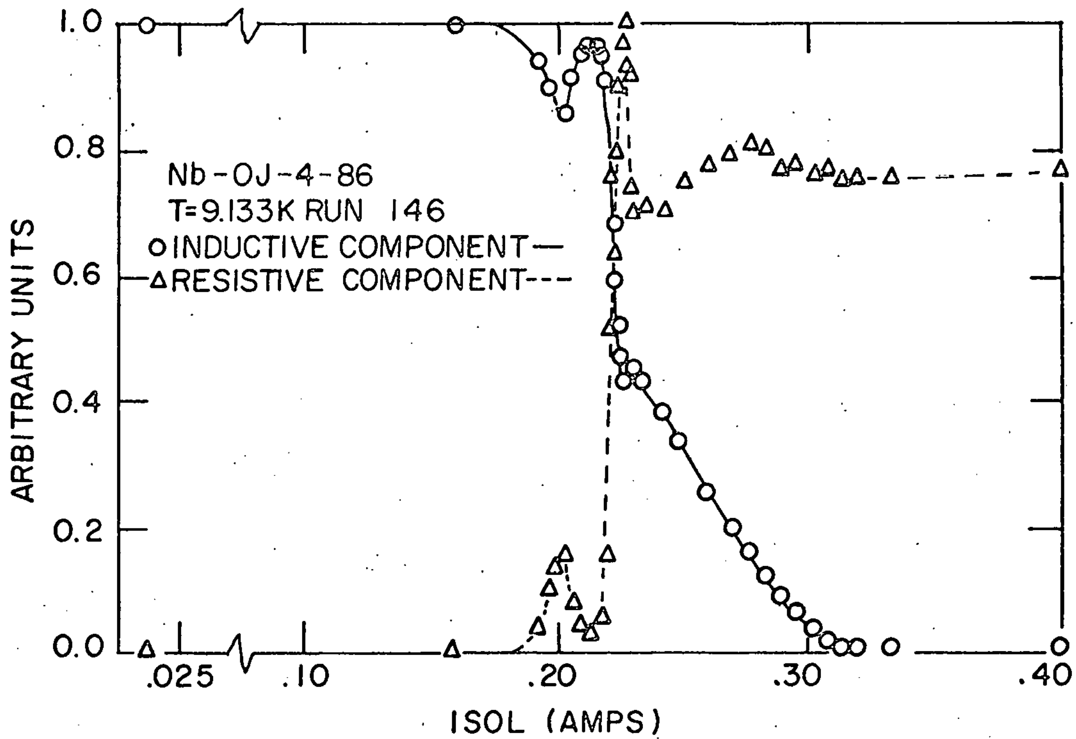

Fig. 17. The real and imaginary susceptibility of niobium at 9.133K

few % less at each reduced temperature. This older sample was one of the samples which was used in the determination of the bulk properties of niobium[11]. Slight shifts which were observed between these samples can probably be attributed to mean free path effects.

Precautions were also taken with regard to field alignment. Webb[10] has reported that if the samples are not perfectly aligned with the field the value of C could be reduced by a few percent. To determine if this was a factor in the results, a field perpendicular to the main field was applied to simulate misalignments up to 2°. As this field was rotated around the main field, measurements of χ' and χ'' were made in the usual manner in the neighborhood of the critical points. There was a shift in the magnitude of the susceptibility values in a sinusoidal manner but to within the error of the measurements the breaks indicating the critical fields did not shift.

In a preliminary publication[14] of this work it was suggested that the large difference between the data and present predictions arose from critical fluctuations but this is certainly not the only possibility. There may be an inhomogeneity in the order parameter as suggested by Clem* and by Hu[13] or there may be a fundamental defect in the effective potential used in the Ginzburg-Landau equation. At this time these proposals are still in the speculative stage.

In an attempt to sort out these possibilities, the data are presented in several ways in an effort to determine if there might be some reasonable empirical form which fits the data or the deviations of the data from the theories. As an initial look at the data we plot $\ell n\, H_{ci}$ vs $\ell n\, \epsilon$ (i = 1, 2, 3) to determine that the data is well behaved in the region of interest.

*Clem, J. R., Department of Physics, Iowa State University of Science and Technology, Ames, Iowa. Inhomogeneous superconductors. Private communication. 1969.

Very good fits are obtained with the scatter being about 1%, 2%, and 5% for H_{c1}, H_{c2}, and H_{c3} respectively (Figs. 18 - 20). From these plots we can write expressions for the critical fields.

Table 1. Critical field fit equations.

Sample	H_{c1}	H_{c2}	H_{c3}
0J-4-85	$2360\epsilon^{0.866}$	$5000\epsilon^{1.024}$	$10,000\epsilon^{1.084}$
0J-4-86	$3000\epsilon^{0.956}$	$4100\epsilon^{0.990}$	$8200\epsilon^{1.074}$

The scatter in H_{c3} of 5% will be the dominant error in the analysis which is to follow. In further measurements this uncertainty will have to be the first problem to be investigated. An expanded view of the critical fields near T_c is shown in Fig. 21.

Over most the temperature range, $t < 0.9$, the theory describes the results fairly well. Hence it would seem reasonable to present the results in terms of deviations from this theory given by $\delta h = 1.695 - C$. Plotting $\ln C$ vs $\ln \epsilon$ (Fig. 22) shows that the data will probably fit some power series expansion in ϵ while $\ln \overline{\delta h}$ vs $\ln \epsilon$ (Fig. 23) gives a smooth fit in ϵ, but the curvature indicates that some changes are still required for a good fit. It is reasonable to determine an expression for $\overline{\delta h}$ as this would simply be a correction term to add to the present expressions which give c as a constant or no more than a slowly varying function of ϵ. Presenting ϵ and $\overline{\delta h}$ in a semi log format (Figs. 24-25) we find that $\ln \epsilon$ vs $\overline{\delta h}$ approaches a straight line for both samples, but the scatter is more than 12%. When we plot $\ln \overline{\delta h}$ vs ϵ the scatter is cut down considerably, however some

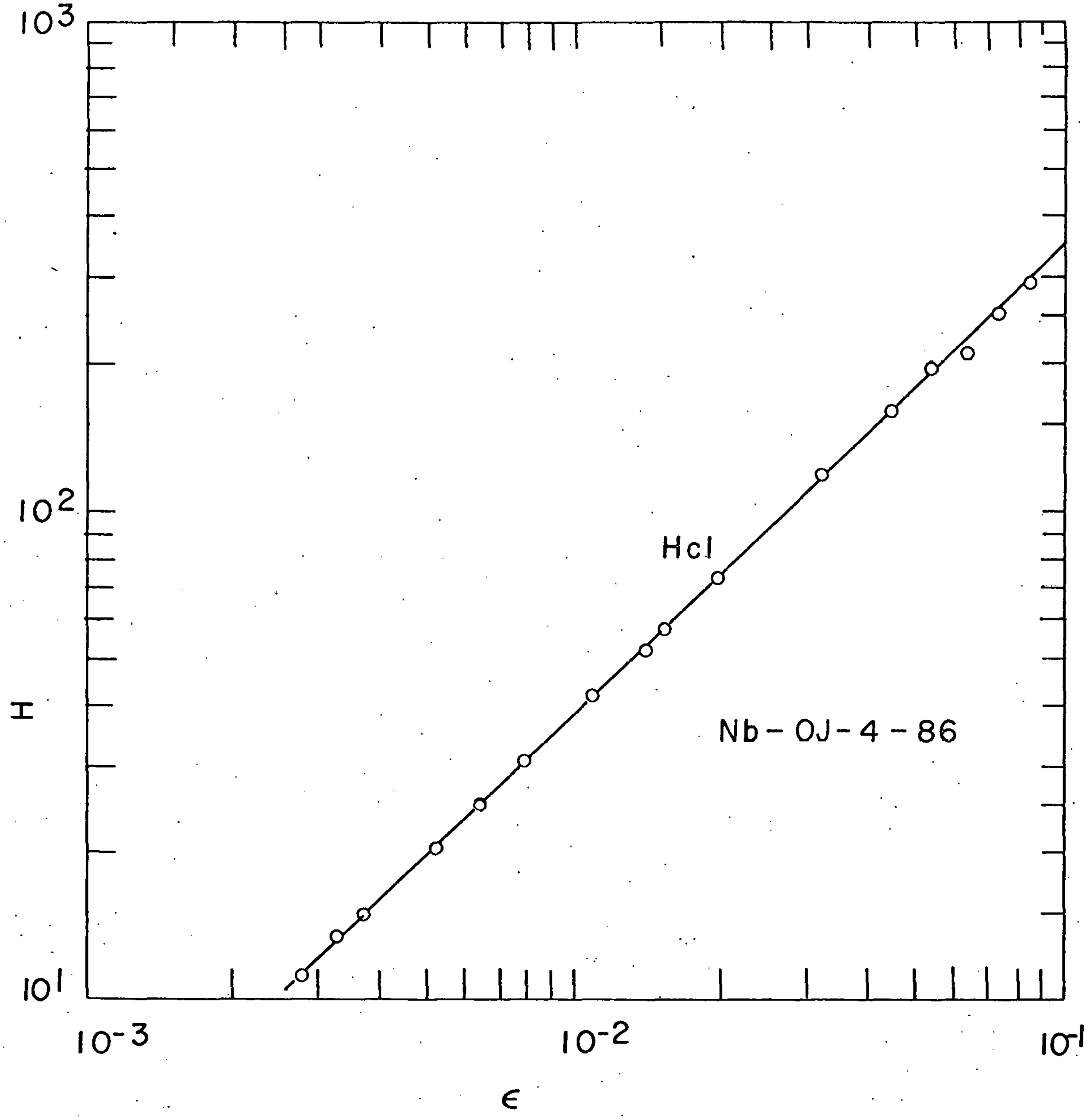

Fig. 18. A plot of $\ell n\ H_{c1}$ vs $\ell n\ \epsilon$

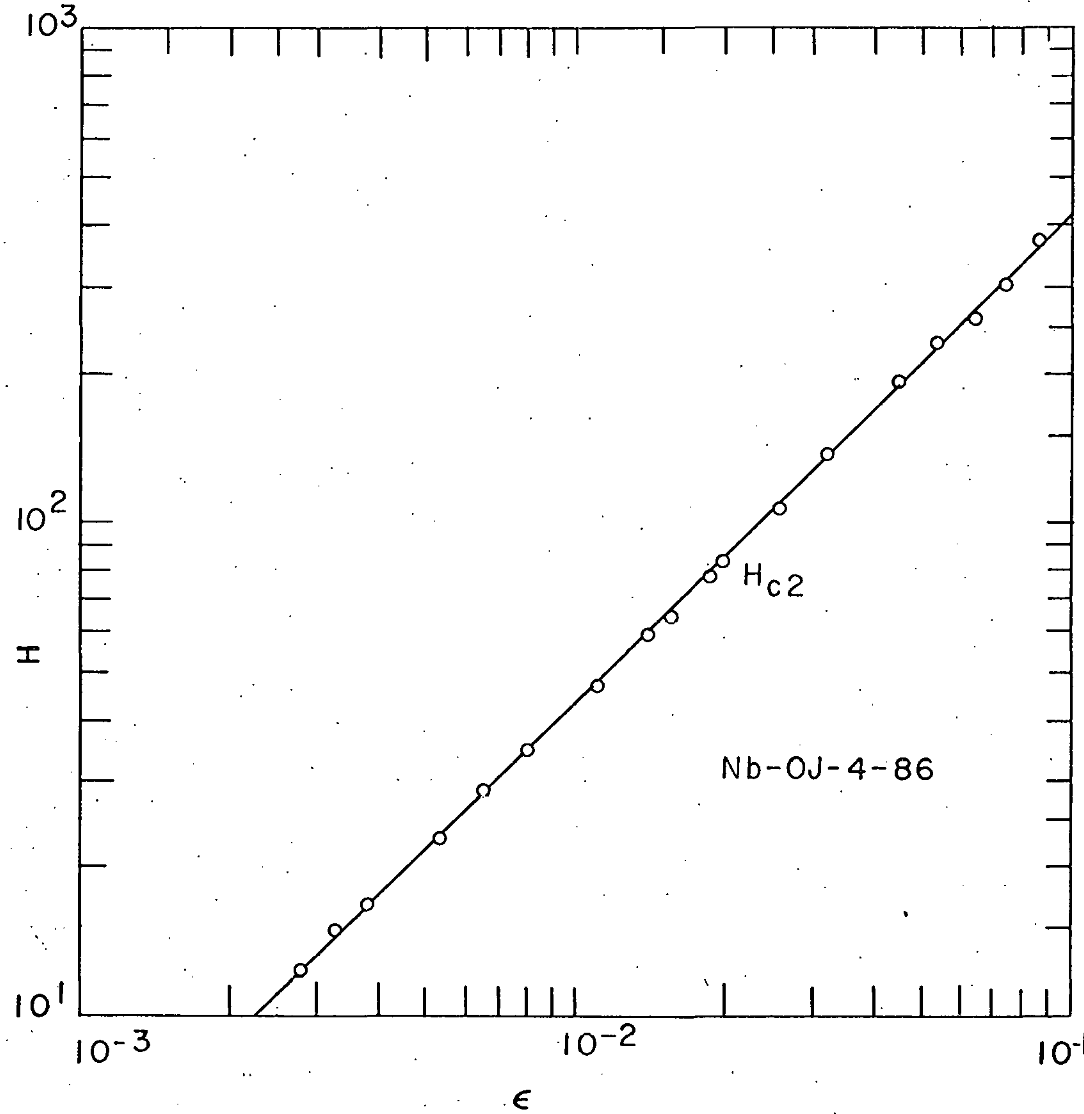

Fig. 19. A plot of $\ell n\ H_{c2}$ vs $\ell n\ \epsilon$

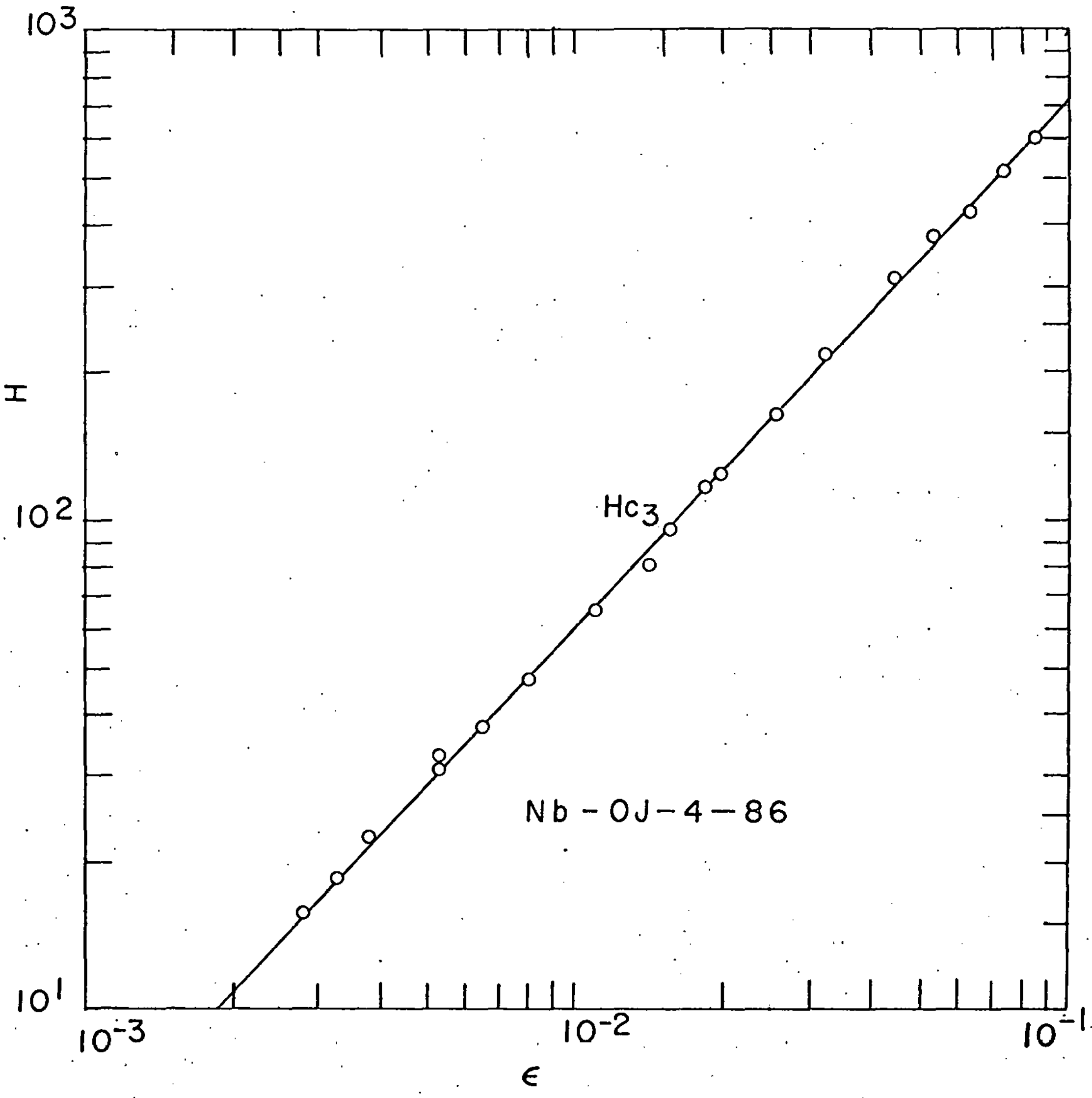

Fig. 20. A plot of $\ell n\ H_{c3}$ vs $\ell n\ \epsilon$

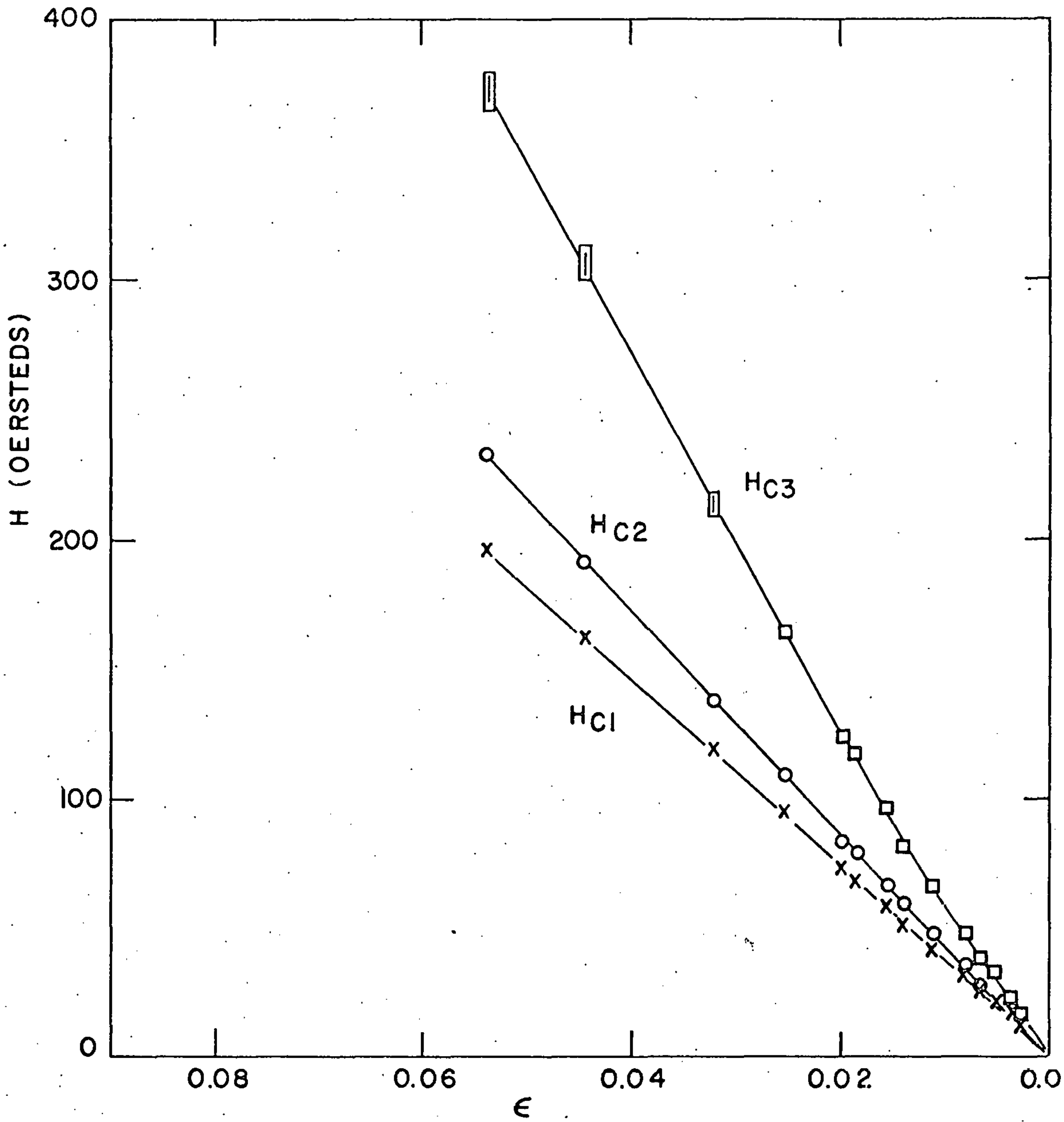

Fig. 21. The experimental phase diagram near T_c

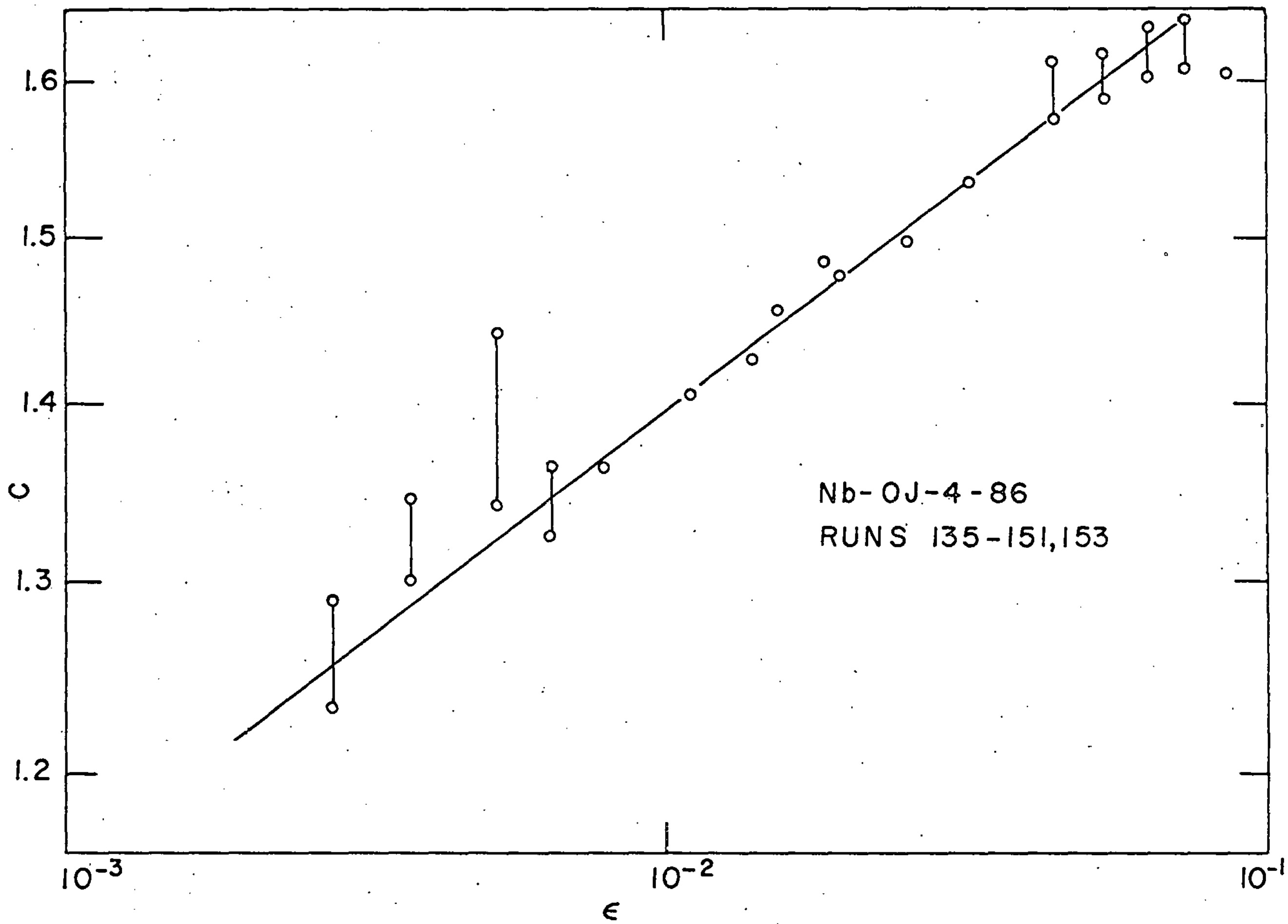

Fig. 22. A plot of ℓn C vs ℓn ϵ

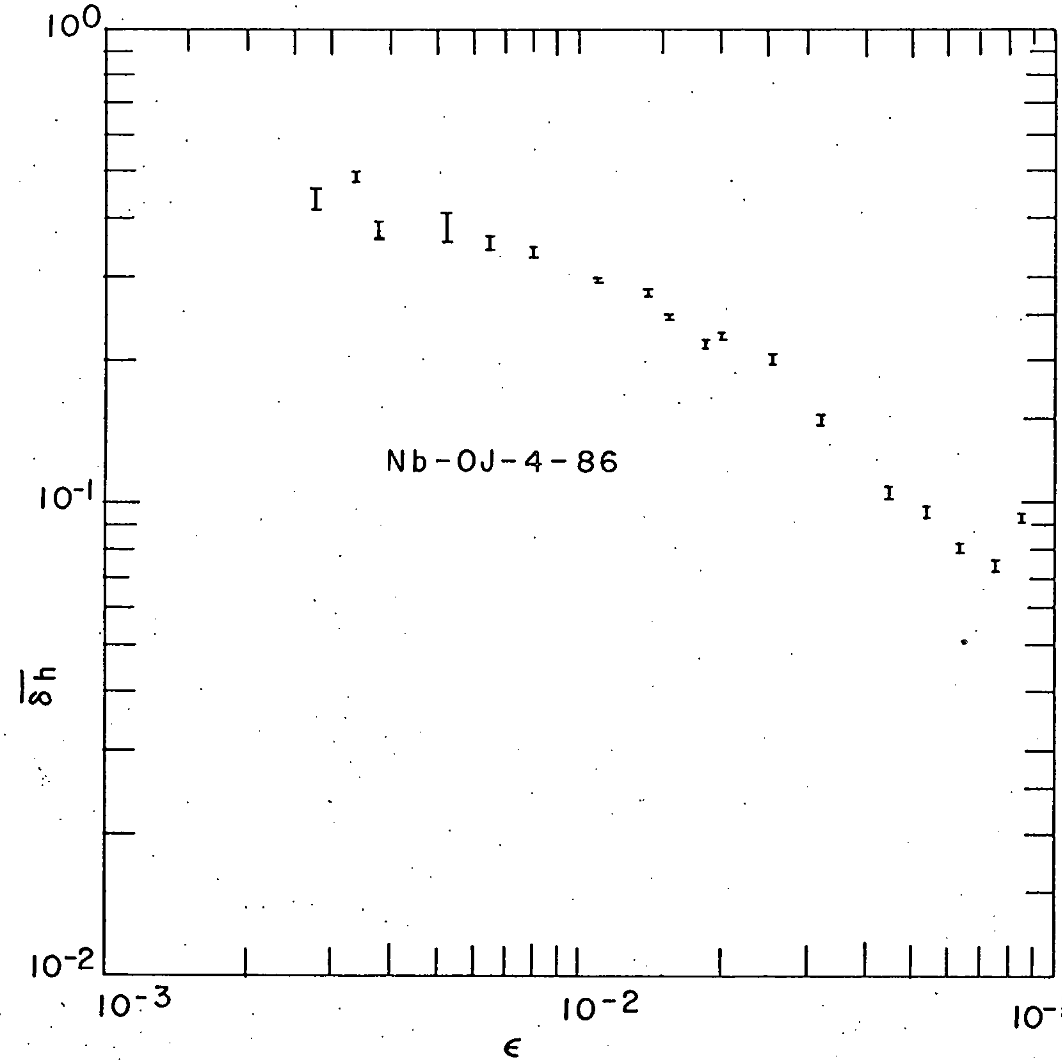

Fig. 23. A plot of $\ell n\ \overline{\delta h}$ vs $\ell n\ \epsilon$

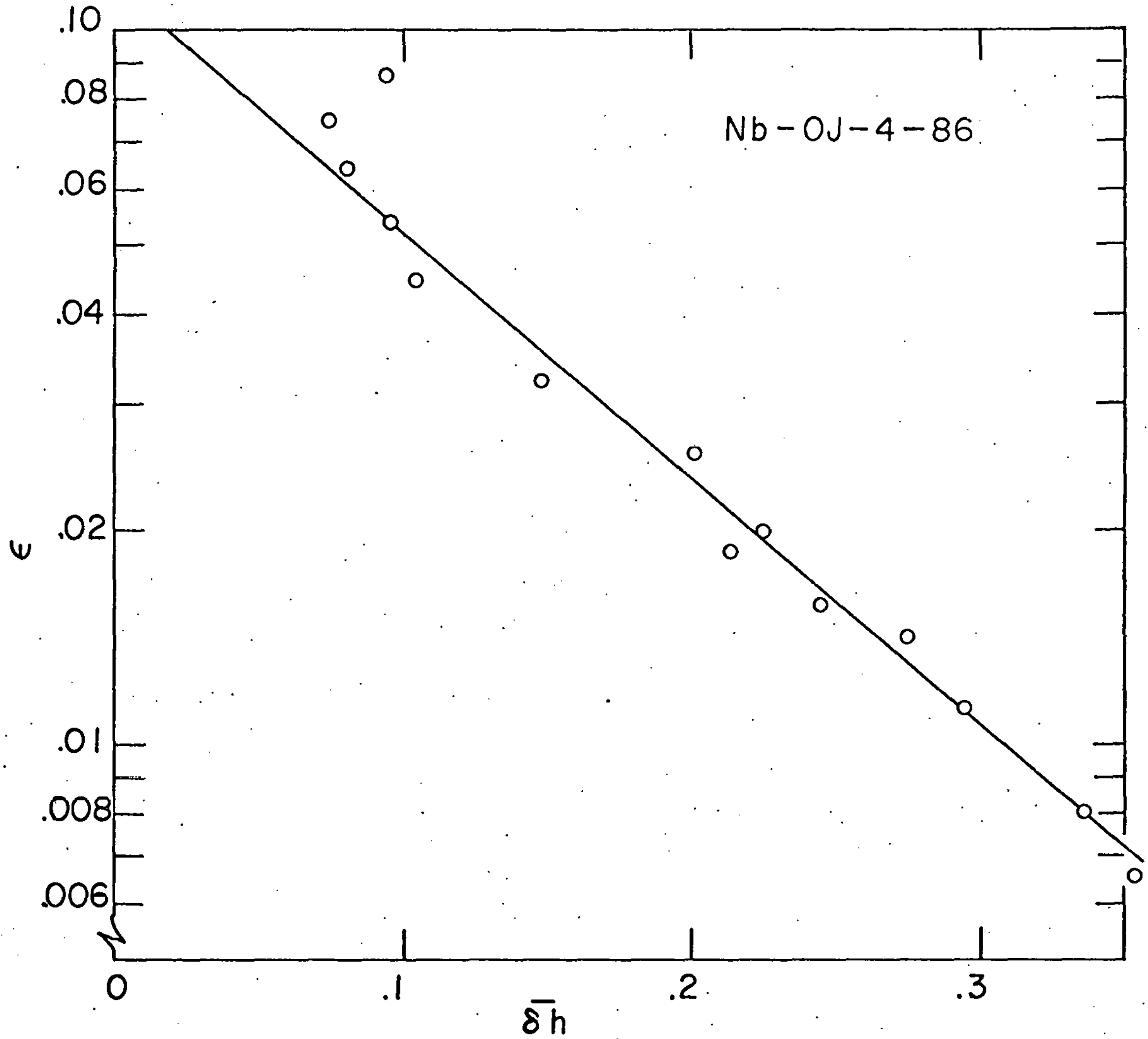

Fig. 24. A plot of ε vs $\overline{\delta h}$

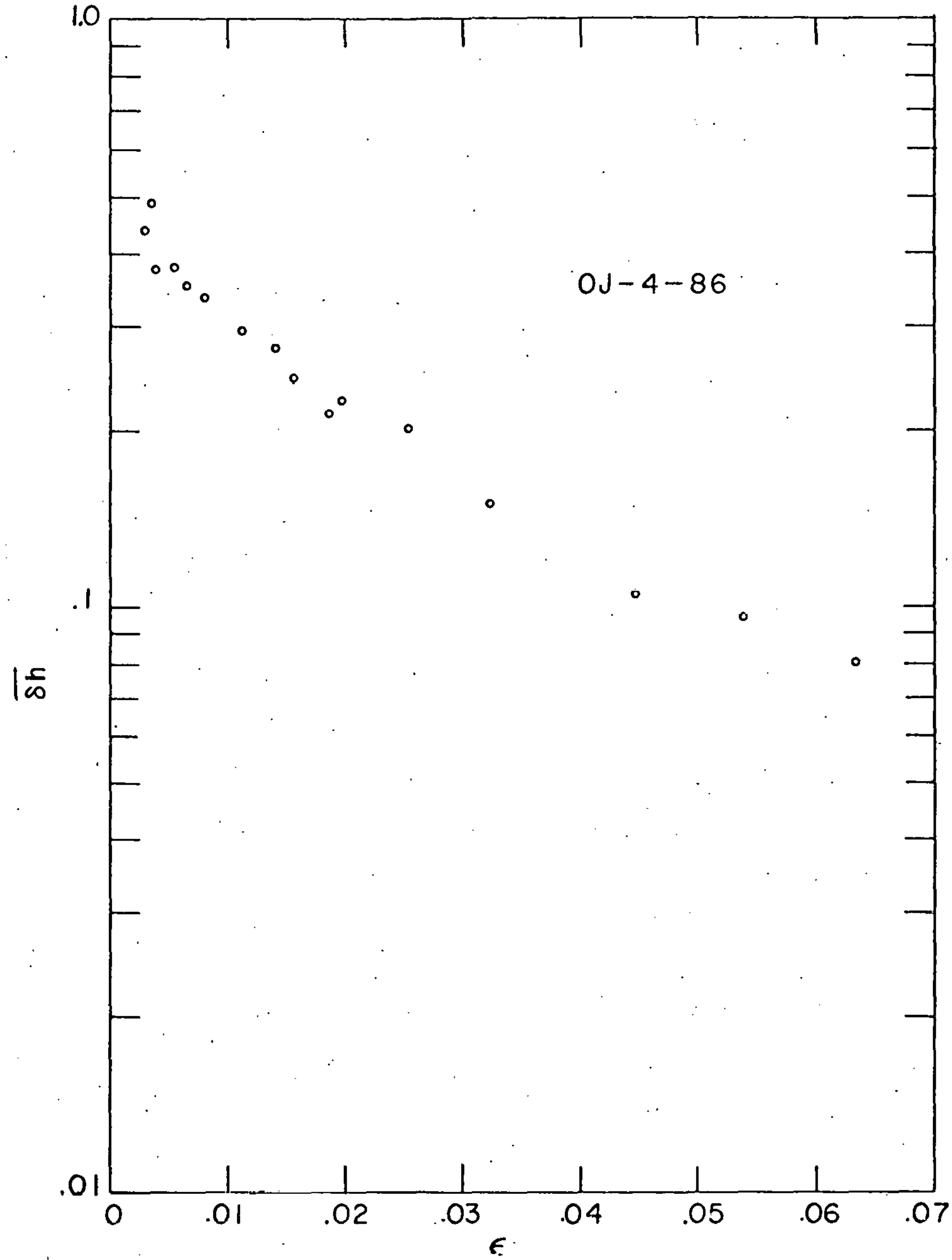

Fig. 25. A plot of $\ell n\ \overline{\delta h}$ vs ϵ

curvature still remains.

If we plot $\ell n\ \overline{\delta h}$ vs $\sqrt{\epsilon}$ (Fig. 26) the curvature disappears and the scatter is on the order of 5% which is determined primarily by the 5% scatter in the H_{c3} data. This would then seem to be the best fit to the data which has been obtained. A least square fit of the data in the region $0.910 < t < 0.997$ gives

$$\overline{\delta h} = 0.696\ e^{-\sqrt{\epsilon/0.014}} \quad . \tag{7}$$

We were pleasantly surprised to find that this expression extrapolates to $C = 1.0$ at $\epsilon = 0$. This difference between the Saint James-de Gennes calculation, as well as other calculations, and the data is huge compared to the experimental uncertainties and must be attributed to some real phenomena.

In Fig. 27 we have presented the values for the reduced order parameter ξ/ξ_o and also a curve of the reduced penetration depth λ/λ. It is readily seen that these parameters are changing very rapidly in the same region where C deviates from a simple slowly varying function. At fields between H_{c2} and H_{c3} the bulk of the specimen is in the normal state with only a small surface sheath being superconducting. The dimension of this sheath is on the order of a coherence distance ξ[5], so in this temperature interval the free energy density can be changing as ξ^{-1}. Within the Ginzburg-Landau (G L)[15] theory the coherence distance ξ may be expressed as

$$\xi = \xi_o\, \epsilon^{-1/2} \tag{8}$$

thus the free energy density would vary as $\epsilon^{+1/2}$. If there now are small fluctuations in the temperature we can consider that the ground state (superconducting) electrons could be excited into the normal state with the probability of this transition being exponential in the free energy density. This leads to an expression

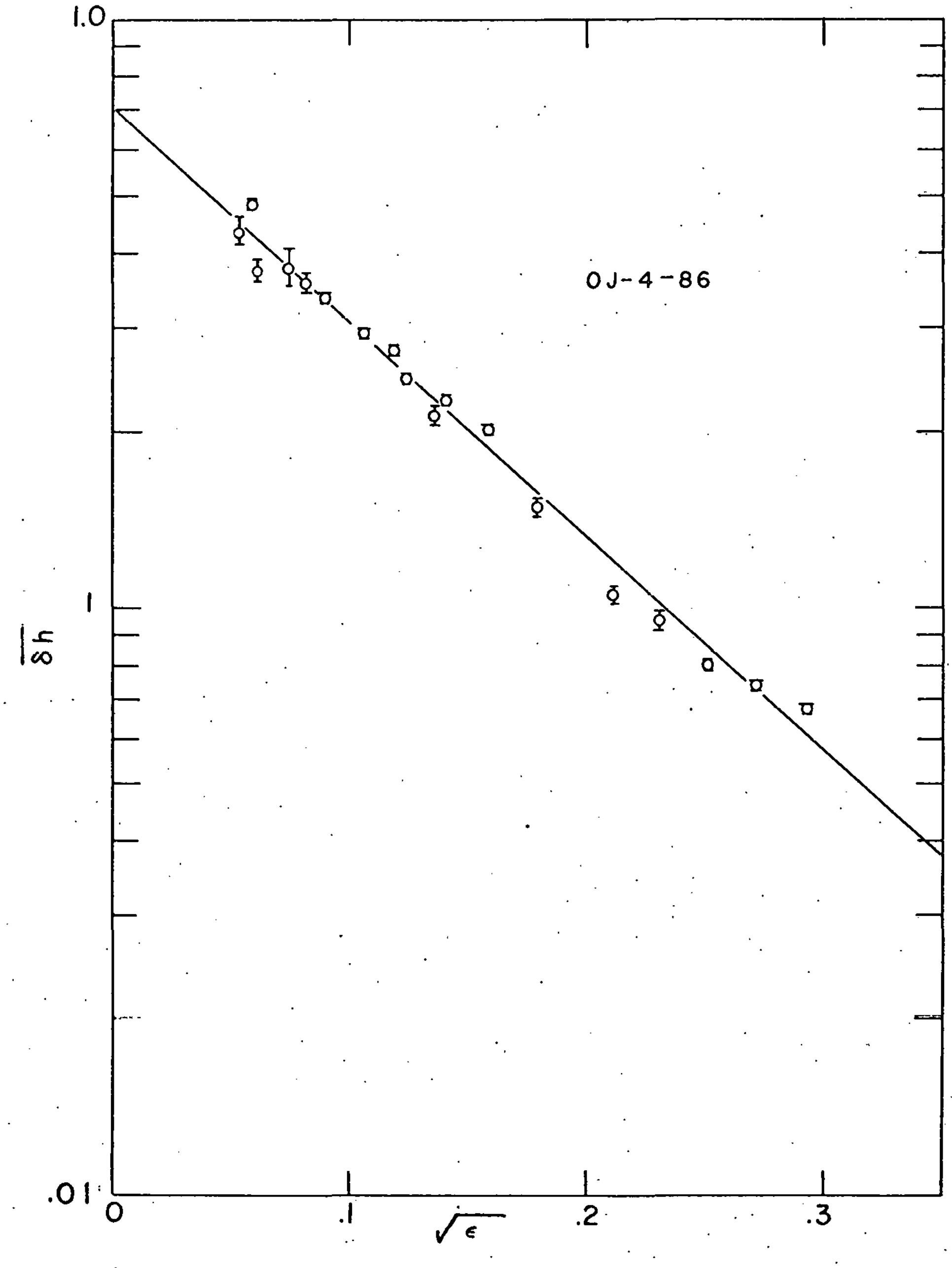

Fig. 26. A plot of $\ln \overline{\delta h}$ vs $\sqrt{\epsilon}$

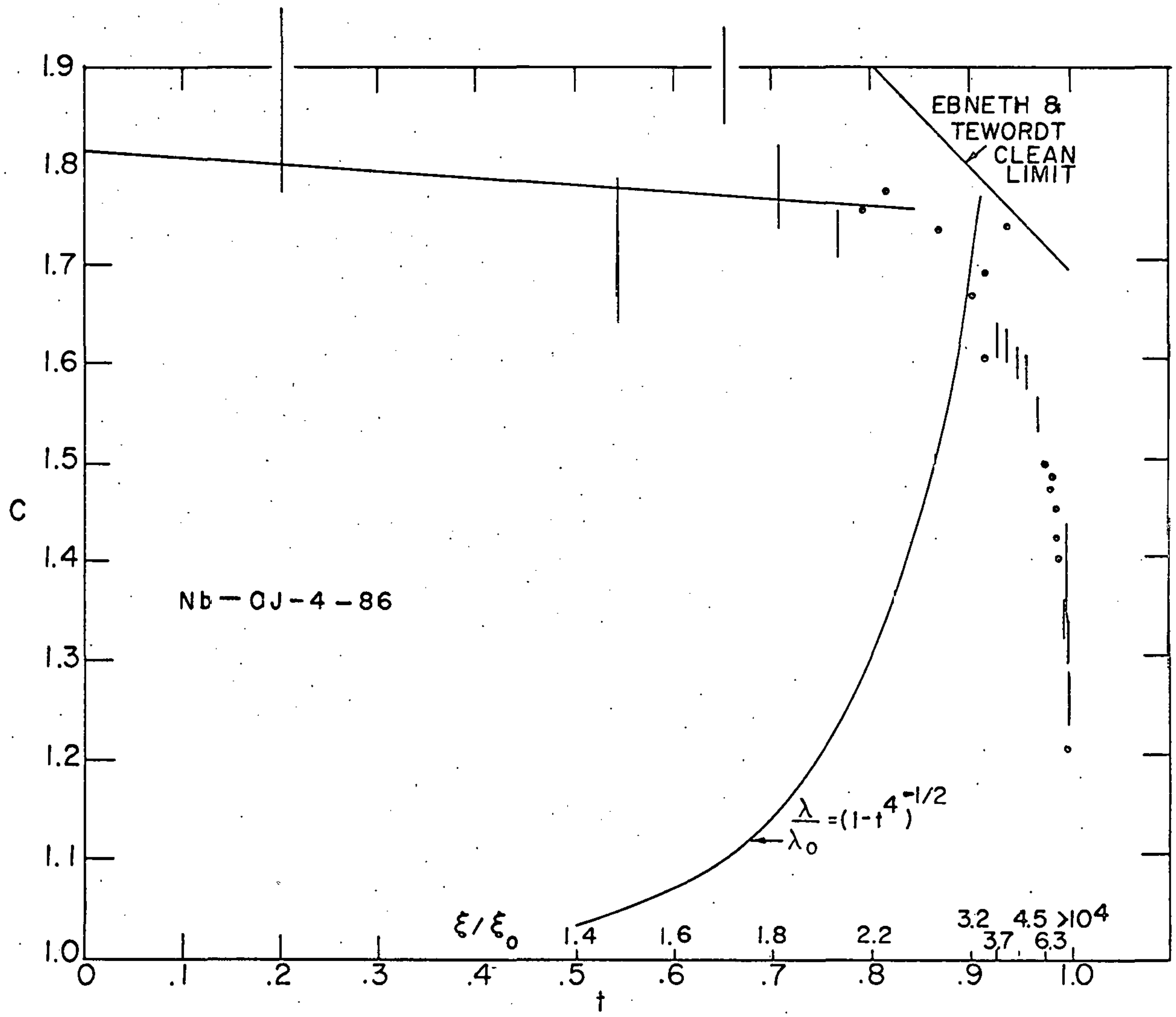

Fig. 27. The plot of C(t) for comparison with the reduced penetration depth and the reduced order parameter

$$\overline{\delta h} = \alpha \ e^{-\beta\sqrt{\epsilon}} \tag{9}$$

which is just the expression which gave the best fit to our data.

In summary there is an extremely large deviation of H_{c3} from the St. James-de Gennes[5] prediction of 1.695 H_{c2} as well as from other expressions such as H K[13] which take into effect more terms of the G L equations and the effect of real surfaces on the boundary conditions. This difference between theory and experiment is very large compared to the experimental uncertainty and must be ascribed to some real phenomena. It has been observed in different samples under various experimental conditions. The most plausible conclusion at this time seems to associate these results with temperature fluctuations. These fluctuations are generally held to be the dominant source of all types of special characteristics which appear near critical points in many different types of critical phenomena[16].

BIBLIOGRAPHY

1. Onnes, H. K., Commun. Kammerlingh Onnes Lab. Univ. Leiden Suppl. 346, 55 (1913).

2. Meissner, W., and R. Ochsenfeld, Naturwissenschaften 21, 787 (1933).

3. Abrikosov, A. A., Soviet Physics JETP 5, 1174 (1957).

4. Goodman, B. B., Phys. Rev. Letters 6, 597 (1961).

5. St. James, D., and P. G. de Gennes, Phys. Letters 7, 306 (1963).

6. Hempstead, C. F., and Y. B. Kim, Phys. Rev. Letters 12, 145 (1964).

7. Finnemore, D. K., T. F. Stromberg, and C. A. Swenson, Phys. Rev. 149, 231 (1966).

8. Ebneth, G., and L. Tewordt, Z. Physik 185, 421 (1965).

9. Lüders, G., Z. Physik 202, 8 (1967).

10. Webb, G. W., Solid State Comm. 6, 33 (1968).

11. Stromberg, T. F., The Superconducting Properties of High Purity Niobium. Unpublished Ph.D. thesis. Ames, Iowa, Library, Iowa State University of Science and Technology. 1965.

12. Anderson, J. W., Anisotropy of the Superconducting Energy Gap in Thorium, Unpublished M.S. thesis. Ames, Iowa, Library, Iowa State University of Science and Technology. 1968.

13. Hu, C. R., and K. Korenman, (To be published in Phys. Rev. ca. 1969).

14. Ostenson, J. E. and D. K. Finnemore, Phys. Rev. Letters 22, 188 (1969).

15. Ginzburg, V. L., and L. D. Landau, Zh. Eksperim. i Theor. Fiz (USSR), 20, 1064 (1950).

16. Kadanoff, L. P., W. Götze, D. Hamblen, R. Hecht, E. Lewis, V. Palciauskas, M. Rayl, J. Swift, D. Aspnes, and J. Kane, Rev. Mod. Phys. 39, 395 (1966).

ACKNOWLEDGMENTS

The author wishes to thank Dr. D. K. Finnemore for suggesting the work presented here and for his continuing interest and advice throughout the entire investigation. Special thanks go to Mr. F. A. Schmidt for providing the high purity niobium for the samples used in these measurements. Financial assistance from the Veterans Administration was greatly appreciated also.

The author would also like to express his appreciation to Dr. Carl Bailey of Concordia College for his introduction to research work while an undergraduate.

APPENDIX

Presented here is the data in its original form. The applied magnetic field is given by

$$H = 150.9\ (\text{ISOL}) \qquad (10)$$

χ' and χ'' were determined from the readout of the ratio transformer (M) and the resistive network (R). χ' is directly proportional to M in arbitrary units. The maximum value of M corresponds to the completely superconducting state while the minimum value indicates the completely normal condition. χ'' in arbitrary units is proportional to 1/(11110000-R). R is a minimum in the superconducting state and the maximum in R appears either at H_{c2} or when the sample is in the completely normal state.

Table 2. Original data.

Sample Nb-OJ-4-85 Run No. 55 T = 6.304K

ISOL	M	R
0.000	52959	11053362
0.000	52956	11053448
1.000	52955	11053455
2.000	52955	11053460
3.000	52955	11053460
4.000	52953	11053502
4.500	52952	11053458
5.000	52950	11053545
5.000	52949	11053630
5.500	52937	11053814
6.000	52872	11055380
6.250	52785	11057342
6.500	52629	11062630
6.750	52832	11056645
7.000	52826	11056925
7.500	52764	11058888
8.000	52732	11060000
8.500	52694	11061076
9.000	52646	11063244
9.250	52606	11065430
9.500	52511	11068772
9.750	52334	11072395
10.000	52108	11074716
10.000	52108	11074670
10.250	51730	11075967
10.500	51711	11074197
10.750	51686	11074255
11.000	51672	11074330
11.000	51670	11074284
11.500	51640	11074311
12.000	51613	11074393
13.000	51563	11074356
14.000	51522	11074320
15.000	51490	11074264
16.000	51461	11074200
17.000	51438	11074142
18.000	51417	11074110
19.000	51405	11074054
20.000	51396	11074062
23.000	51375	11074180
26.000	51357	11074254
30.000	51333	11074435

Table 2. Continued.

Sample Nb-OJ-4-85		Run No. 56		T = 7.016K	
ISOL	M	R	ISOL	M	R
0.000	52957	11053464	7.000	52500	11069495
0.000	52955	11053407	7.000	52492	11069694
0.500	52954	11053407	7.100	52395	11071825
1.000	52954	11053407	7.200	52282	11073490
1.500	52954	11053407	7.300	52150	11074803
2.000	52954	11053420	7.400	52010	11075807
2.500	52954	11053436	7.500	51746	11076805
3.000	52953	11053450	7.500	51735	11076810
3.500	52951	11053510	7.700	51711	11074228
4.000	52946	11053641	7.900	51688	11074292
4.300	52937	11053925	8.000	51678	11074310
4.500	52917	11054335	8.500	51637	11074350
4.600	52903	11054783	9.000	51602	11074322
4.800	52827	11056452	9.500	51570	11074290
5.000	52611	11061874	10.000	51541	11074240
5.000	52605	11062130	10.500	51517	11074190
5.200	52721	11059575	11.000	51498	11074138
5.400	52903	11057694	11.500	51478	11074069
5.500	52800	11057800	12.000	51462	11074034
5.600	52791	11058122	12.500	51449	11073980
5.800	52768	11059010	13.000	51437	11073930
6.000	52732	11060100	13.500	51426	11073880
6.500	52666	11062575	14.000	51422	11073865
6.600	52651	11063255	15.000	51416	11073913
6.300	52603	11065592	17.000	51404	11073952

Table 2. Continued.

Sample Nb-OJ-4-85		Run No. 57		T = 7.824K	
ISOL	M	R	ISOL	M	R
0.000	52962	11053585	4.800	51685	11074365
1.000	52961	11053612	4.900	51670	11074370
2.000	52959	11053682	5.000	51656	11074382
3.000	52903	11055020	5.000	51653	11074290
3.000	52885	11055504	5.100	51642	11074381
3.100	52858	11056096	5.200	51631	11074380
3.200	52788	11057780	5.300	51620	11074366
3.300	52624	11062394	5.400	51610	11074370
3.400	52440	11068459	5.500	51600	11074355
3.500	52735	11060362	5.600	51590	11074345
3.600	52764	11059904	5.700	51578	11074332
3.700	52746	11060528	5.800	51569	11074310
3.800	52720	11061635	5.900	51559	11074287
3.900	52696	11062570	6.000	51551	11074269
4.000	52691	11063059	6.000	51551	11074305
4.000	52669	11063778	7.000	51485	11074080
4.100	52634	11065348	8.000	51447	11073874
4.200	52565	11068240	8.000	51446	11073825
4.300	52442	11072137	9.000	51440	11073870
4.400	52243	11075400	10.000	51436	11073842
4.500	51992	11077410	10.000	51435	11073885
4.600	51649	11076370	12.000	51429	11073880
4.700	51705	11074336	15.000	51417	11073956

Table 2. Continued.

Sample Nb-OJ-4-85			Run No. 58A	T = 8.216 K	
ISOL	M	R	ISOL	M	R
0.000	52962	11053645	3.440	51688	11074540
0.500	52962	11053645	3.460	51686	11074462
1.000	52961	11053675	3.480	51681	11074450
1.500	52960	11053752	3.500	51676	11074440
1.800	52953	11053895	3.500	51676	11074425
2.000	52942	11054165	3.520	51672	11074435
2.100	52932	11054448	3.540	51667	11074425
2.200	52912	11054964	3.600	51655	11074416
2.300	52870	11056012	3.700	51636	11074418
2.400	52794	11057926	3.800	51621	11074412
2.500	52622	11062625	3.900	51607	11074403
2.600	52185	11074172	4.000	51594	11074372
2.700	52696	11062483	4.300	51556	11074303
2.800	52720	11062157	4.600	51523	11074192
2.900	52687	11063419	4.900	51498	11074080
3.000	52645	11065567	5.300	51471	11073940
3.100	52560	11069234	5.600	51457	11073852
3.200	52351	11074782	5.900	51449	11073800
3.300	52016	11078158	6.200	51447	11073806
3.300	52075	11077769	6.500	51446	11073803
3.320	51994	11078283	6.800	51445	11073810
3.340	51900	11078763	7.100	51444	11073819
3.360	51726	11079532	7.600	51442	11073808
3.380	51632	11079317	8.000	51441	11073816
3.400	51660	11075340	9.000	51438	11073828
3.400	51613	11076815	10.000	51435	11073852
3.420	51664	11075124			

Table 2. Continued.

Sample Nb-OJ-4-85			Run No. 59	T = 8.726 K	
ISOL	M	R	ISOL	M	R
0.000	52954	11053648	1.430	52321	11076665
0.400	52954	11053648	1.440	52274	11077299
0.600	52953	11053700	1.450	52213	11078012
0.700	52952	11053760	1.450	52201	11078142
0.800	52948	11053845	1.460	52145	11078638
0.900	52942	11054035	1.470	52063	11079350
1.000	52928	11054392	1.480	52024	11079625
1.000	52926	11054515	1.490	51861	11080512
1.050	52913	11054823	1.500	51576	11081113
1.080	52897	11055255	1.500	51547	11080653
1.100	52873	11055905	1.510	51520	11079595
1.110	52870	11055960	1.520	51536	11077758
1.130	52848	11056540	1.530	51585	11076142
1.150	52819	11057370	1.540	51627	11075100
1.170	52777	11058478	1.550	51633	11074846
1.190	52721	11060038	1.550	51634	11074845
1.200	52658	11062035	1.575	51625	11074690
1.210	52634	11062792	1.600	51616	11074615
1.220	52572	11064826	1.650	51601	11074520
1.230	52506	11067152	1.700	51582	11074463
1.240	52449	11069675	1.750	51566	11074400
1.250	52399	11071927	1.800	51554	11074361
1.260	52378	11073100	1.850	51538	11074310
1.270	52433	11072140	1.900	51526	11074255
1.280	52470	11071506	1.950	51513	11074192
1.290	52522	11070451	2.000	51506	11074155
1.300	52535	11070283	2.000	51505	11074125
1.300	52569	11069550	2.100	51486	11074020
1.310	52540	11070360	2.200	51472	11073935
1.320	52543	11070700	2.300	51460	11073855
1.330	52551	11070814	2.400	51451	11073779
1.340	52541	11071182	2.500	51446	11073750
1.350	52535	11071460	2.600	51445	11073742
1.350	52527	11071819	2.700	51445	11073754
1.360	52507	11072300	2.800	51444	11073748
1.370	52486	11073122	3.000	51443	11073740
1.380	52470	11073574	3.000	51443	11073770
1.390	52449	11074122	3.250	51442	11073750
1.400	52431	11074680	3.500	51441	11073740
1.400	52429	11074726	3.750	51441	11073740
1.410	52394	11075524	4.000	51441	11073740
1.420	52361	11076076	4.000	51441	11073765

Table 2. Continued.

	Sample Nb-0J-4-85		Run No. 60	T = 8.934 K	
ISOL	M	R	ISOL	M	R
0.000	52955	11053708	0.975	51534	11074346
0.200	52955	11053708	1.000	51522	11074275
0.300	52954	11053745	1.000	51509	11074182
0.500	52946	11054009	1.050	51503	11074146
0.500	52943	11054080	1.100	51485	11074030
0.525	52942	11054120	1.100	51475	11073960
0.550	52936	11054304	1.150	51471	11073950
0.575	52926	11054592	1.200	51462	11073874
0.600	52910	11055100	1.200	51462	11073868
0.600	52884	11055758	1.200	51455	11073803
0.625	52873	11056060	1.225	51458	11073837
0.650	52804	11057982	1.250	51454	11073815
0.675	52633	11063094	1.250	51454	11073809
0.700	52406	11072261	1.275	51452	11073784
0.700	52474	11074850	1.300	51450	11073768
0.725	52510	11074668	1.300	51448	11073772
0.750	52446	11076980	1.350	51449	11073761
0.775	52248	11079574	1.400	51448	11073767
0.800	51998	11081242	1.400	51446	11073770
0.800	51483	11081166	1.450	51448	11073765
0.825	51481	11080804	1.500	51447	11073760
0.850	51562	11075798	1.500	51445	11073760
0.875	51582	11074856	1.600	51445	11073760
0.900	51569	11074660	1.800	51443	11073752
0.900	51554	11074500	2.000	51442	11073758
0.925	51557	11074519	3.000	51441	11073758
0.950	51546	11074424			

2

Table 2. Continued.

Sample Nb-OJ-4-85		Run No. 65		T = 8.994 K	
ISOL	M	R	ISOL	M	R
0.000	52953	11053631	0.580	52362	11079222
0.100	52953	11053631	0.580	52327	11079832
0.200	52953	11053677	0.585	52313	11079838
0.300	52950	11053750	0.590	52251	11080340
0.350	52945	11053882	0.595	52190	11080873
0.360	52947	11053800	0.600	52099	11081518
0.400	52936	11054151	0.600	52062	11081868
0.410	52939	11054047	0.605	52010	11081984
0.430	52933	11054190	0.610	51951	11082229
0.450	52924	11054475	0.615	51920	11082379
0.450	52906	11055100	0.620	51800	11082950
0.470	52904	11054976	0.620	51900	11082653
0.480	52890	11055445	0.625	51757	11082864
0.490	52863	11056100	0.630	51492	11082873
0.495	52849	11056508	0.635	51431	11081860
0.500	52830	11057030	0.640	51409	11080499
0.500	52723	11060053	0.640	51433	11079802
0.505	52803	11057772	0.645	51413	11079440
0.510	52763	11058978	0.650	51428	11078265
0.515	52715	11060404	0.655	51456	11077203
0.520	52654	11062311	0.660	51493	11076145
0.520	52516	11066765	0.660	51537	11075700
0.525	52592	11064364	0.665	51521	11075372
0.530	52530	11066683	0.670	51538	11074970
0.535	52451	11069498	0.675	51538	11074837
0.540	52413	11071363	0.680	51555	11074832
0.540	52293	11075156	0.680	51536	11074736
0.545	52375	11073692	0.685	51534	11074680
0.550	52480	11074760	0.695	51531	11074613
0.550	52356	11075572	0.695	51529	11074563
0.555	52367	11076578	0.700	51527	11074529
0.560	52496	11077042	0.700	51545	11074639
0.560	52367	11077545	0.720	51534	11074461
0.565	52376	11078170	0.740	51523	11074345
0.570	52378	11078380	0.760	51512	11074265
0.570	52463	11078400	0.780	51502	11074170
0.575	52376	11078850	0.800	51491	11074105

Table 2. Continued.

Sample Nb-OJ-4-85	Run No. 65	T = 8.994 K
ISOL	M	R
0.820	51483	11074034
0.840	51475	11073975
0.860	51469	11073934
0.880	51463	11073885
0.900	51460	11073847
0.920	51455	11073823
0.940	51451	11073799
0.960	51449	11073765
0.980	51447	11073742
1.000	51447	11073742
1.020	51446	11073740
1.060	51445	11073740
1.100	51445	11073740
1.300	51442	11073744
1.500	51441	11073725

Table 2. Continued.

Sample Nb-OJ-4-85		Run No. 66		T = 7.665 K	
ISOL	M	R	ISOL	M	R
0.000	52961	11053766	5.150	51658	11077562
0.500	52961	11053766	5.200	51696	11074800
1.000	52961	11053766	5.250	51708	11074366
1.500	52960	11053801	5.300	51700	11074401
2.000	52958	11053820	5.350	51691	11074405
2.500	52955	11053908	5.400	51683	11074401
2.700	52951	11054000	5.500	51670	11074422
2.900	52944	11054173	5.600	51657	11074417
3.100	52930	11054542	5.700	51646	11074426
3.300	52887	11055596	5.800	51636	11074429
3.400	52844	11056604	5.900	51626	11074424
3.500	52777	11058273	6.000	51617	11074446
3.600	52640	11061828	6.100	51608	11074429
3.650	52680	11060518	6.200	51600	11074426
3.700	52464	11067108	6.300	51591	11074401
3.700	52310	11071400	6.400	51582	11074401
3.750	52377	11069903	6.500	51573	11074379
3.800	52511	11065672	6.500	51543	11074213
3.850	52696	11061358	6.600	51538	11074213
3.900	52760	11059875	6.700	51533	11074200
3.950	52771	11059660	6.800	51528	11074200
4.000	52770	11059800	6.900	51523	11074180
4.050	52764	11059975	7.000	51518	11074177
4.100	52754	11060114	7.000	51534	11074274
4.150	52750	11060420	7.200	51521	11074250
4.200	52736	11061000	7.400	51510	11074215
4.250	52726	11061410	7.600	51500	11074160
4.300	52714	11061914	7.800	51490	11074111
4.350	52705	11062320	8.000	51480	11074069
4.400	52696	11062760	8.200	51472	11074042
4.450	52685	11063224	8.300	51468	11074036
4.500	52676	11063712	8.400	51465	11074025
4.550	52661	11064407	8.500	51462	11074000
4.600	52646	11065180	8.600	51458	11073983
4.660	52622	11066321	8.300	51453	11073953
4.700	52600	11067404	8.700	51455	11073972
4.750	52560	11069030	8.900	51450	11073932
4.800	52494	11071184	9.000	51447	11073922
4.850	52415	11072954	9.200	51444	11073900
4.900	52327	11074465	9.400	51443	11073905
4.950	52230	11075635	9.600	51441	11073892
5.000	52125	11076564	9.800	51441	11073900
5.050	52016	11077295	10.000	51441	11073900
5.100	51782	11078324	11.000	51435	11073900

Table 2. Continued.

Sample Nb-0J-4-85		Run No. 67		T = 8.261 K	
ISOL	M	R	ISOL	M	R
0.000	52962	11053795	3.350	51631	11074449
0.500	52962	11053795	3.400	51623	11074441
1.000	52962	11053795	3.500	51607	11074420
1.500	52959	11053897	3.600	51592	11074410
1.800	52950	11054157	3.700	51577	11074387
2.000	52925	11054830	3.800	51563	11074343
2.200	52809	11057708	3.900	51551	11074312
2.300	52609	11063674	4.000	51538	11074259
2.350	52411	11070293	4.100	51527	11074211
2.400	52549	11067055	4.200	51516	11074182
2.450	52651	11064516	4.300	51507	11074132
2.500	52683	11063800	4.400	51500	11074090
2.550	52689	11063810	4.500	51491	11074049
2.600	52660	11065037	4.600	51483	11074010
2.650	52634	11066095	4.700	51477	11073980
2.700	52620	11067140	4.800	51471	11073930
2.750	52573	11068907	4.900	51465	11073891
2.800	52510	11071396	5.000	51461	11073870
2.850	52400	11074330	5.100	51456	11073837
2.900	52235	11076715	5.200	51453	11073804
2.950	52033	11078310	5.300	51453	11073814
3.000	51726	11079882	5.400	51453	11073816
3.050	51662	11075424	5.500	51452	11073816
3.100	51691	11074534	5.600	51452	11073816
3.150	51675	11074490	6.000	51450	11073830
3.200	51662	11074467	6.500	51448	11073842
3.250	51651	11074451	7.000	51446	11073842
3.300	51641	11074455	8.000	51444	11073865

Table 2. Continued.

	Sample Nb-OJ-4-85		Run No. 68	T = 8.549 K	
ISOL	M	R	ISOL	M	R
0.000	52962	11053745	2.025	51662	11074749
0.500	52962	11053770	2.050	51654	11074670
1.000	52958	11058884	2.075	51644	11074595
1.200	52950	11054141	2.100	51636	11074555
1.400	52912	11055214	2.150	51622	11074500
1.500	52828	11057324	2.200	51608	11074470
1.525	52787	11058426	2.250	51595	11074441
1.550	52731	11059915	2.300	51583	11074401
1.575	52649	11062547	2.350	51572	11074381
1.600	52504	11067454	2.400	51562	11074367
1.625	52402	11071843	2.450	51551	11074318
1.650	52483	11070410	2.500	51541	11074290
1.675	52571	11068640	2.550	51532	11074255
1.700	52597	11068010	2.600	51523	11074220
1.725	52604	11067877	2.650	51514	11074166
1.750	52602	11068247	2.700	51508	11074132
1.775	52573	11069426	2.800	51494	11074070
1.800	52543	11070567	2.900	51481	11073978
1.825	52513	11071855	3.000	51472	11073925
1.850	52460	11073670	3.100	51464	11073880
1.875	52371	11075603	3.200	51457	11073822
1.900	52263	11077155	3.300	51453	11073780
1.925	52110	11078660	3.400	51453	11073797
1.950	51880	11080075	3.500	51452	11073797
1.975	51562	11079710	3.700	51451	11073797
2.000	51623	11075771	4.000	51450	11073797

Table 2. Continued.

	Sample No. Nb-OJ-4-85		Run No. 69	T = 9.001 K	
ISOL	M	R	ISOL	M	R
0.000	52954	11053770	0.540	51450	11080755
0.050	52954	11053770	0.545	51470	11078808
0.100	52954	11053795	0.550	51490	11077690
0.150	52954	11053803	0.555	51520	11076646
0.200	52953	11053844	0.560	51549	11075669
0.250	52951	11053920	0.565	51565	11075288
0.300	52946	11054064	0.570	51565	11075141
0.350	52932	11054520	0.575	51563	11075046
0.360	52926	11054706	0.580	51560	11074957
0.370	52916	11055000	0.585	51557	11074900
0.380	52902	11055495	0.590	51553	11074790
0.390	52877	11056230	0.595	51547	11074710
0.395	52865	11056472	0.600	51544	11074686
0.400	52842	11057100	0.610	51535	11074590
0.405	52822	11057645	0.620	51528	11074500
0.410	52797	11058251	0.630	51521	11074421
0.415	52754	11059478	0.640	51514	11074350
0.420	52712	11061010	0.650	51507	11074295
0.425	52656	11062700	0.660	51502	11074240
0.430	52611	11064301	0.670	51495	11074184
0.435	52535	11066997	0.680	51490	11074152
0.440	52465	11069426	0.690	51484	11074105
0.445	52402	11071933	0.700	51479	11074068
0.450	52357	11074003	0.710	51475	11074035
0.455	52359	11075570	0.720	51472	11074000
0.460	52378	11077033	0.730	51470	11073980
0.465	52352	11078358	0.740	51466	11073955
0.470	52421	11078642	0.750	51464	11073932
0.475	52435	11079101	0.760	51461	11073905
0.480	52392	11079910	0.770	51459	11073892
0.488	52318	11080635	0.780	51457	11073869
0.490	52249	11081200	0.790	51456	11073856
0.495	52194	11081662	0.800	51455	11073835
0.500	52137	11082019	0.810	51454	11073835
0.505	52052	11082585	0.820	51453	11073830
0.510	51987	11082816	0.830	51453	11073830
0.515	51949	11083280	0.840	51452	11073830
0.520	51860	11083521	0.850	51452	11073830
0.525	51685	11083685	0.875	51452	11073830
0.530	51550	11083208	0.900	51452	11073830
0.535	51490	11082312			

Table 2. Continued.

	Sample No. Nb-OJ-4-86		Run No. 135	T = 8.416 K	
ISOL	M	R	ISOL	M	R
0.000	52829	11072950	2.470	52268	11080100
0.100	52829	11072950	2.475	52297	11079660
0.200	52829	11072950	2.480	52319	11079230
0.300	52829	11072950	2.485	52319	11079265
0.500	52829	11072950	2.490	52319	11079279
0.800	52829	11072950	2.495	52319	11079145
0.900	52829	11072950	2.500	52312	11079240
1.001	52825	11072890	2.505	52311	11079410
1.683	52804	11073220	2.510	52311	11079258
1.765	52766	11073600	2.515	52311	11079335
1.796	52742	11073650	2.520	52310	11079340
1.833	52706	11074130	2.525	52309	11079384
1.847	52684	11074380	2.530	52305	11079490
1.884	52624	11075062	2.540	52301	11079397
1.900	52614	11075062	2.551	52301	11079474
1.920	52598	11075108	2.577	52293	11079550
1.940	52580	11075542	2.597	52292	11079558
1.960	52590	11075308	2.617	52276	11079611
1.980	52646	11074715	2.649	52270	11079743
2.000	52726	11073820	2.679	52253	11079849
2.020	52766	11073565	2.700	52242	11079820
2.040	52780	11073310	2.751	52222	11079932
2.060	52780	11073310	2.800	52214	11080014
2.080	52780	11073310	2.900	52182	11080275
2.100	52785	11073310	3.000	52143	11080448
2.120	52789	11073310	3.100	52110	11080562
2.140	52780	11073310	3.200	52060	11080859
2.160	52774	11073405	3.303	52018	11080995
2.250	52734	11072787	3.400	51972	11081145
2.374	52664	11074802	3.500	51922	11081208
2.400	52614	11076373	3.600	51868	11081449
2.442	52507	11078232	3.700	51818	11081535
2.460	52307	11080000	3.800	51748	11081490
2.490	52310	11079241	3.905	51701	11081606
2.440	52490	11078555	4.000	51644	11081473
2.445	52440	11078961	4.100	51614	11081333
2.450	52400	11079495	4.204	51614	11081333
2.455	52370	11079685	4.400	51614	11081333
2.460	52330	11079956	5.000	51614	11081333
2.465	52292	11080206			

Table 2. Continued.

Sample No. Nb-OJ-4-86			Run No. 136	T = 8.526 K	
ISOL	M	R	ISOL	M	R
0.100	52830	11072839	2.040	52560	11077356
1.100	52830	11072839	2.050	52400	11079470
1.300	52830	11072839	2.060	52300	11080010
1.500	52790	11073165	2.070	52260	11079923
1.550	52770	11073578	2.080	52310	11079360
1.600	52728	11073708	2.090	52310	11079360
1.650	52643	11074822	2.100	52300	11079380
1.670	52623	11074975	2.150	52280	11079589
1.700	52723	11073920	2.200	52260	11079365
1.720	52743	11073780	2.310	52210	11080156
1.735	52773	11073481	2.420	52160	11080390
1.770	52773	11073481	2.604	52070	11080740
1.800	52773	11073481	2.800	51971	11081300
1.850	52773	11073481	3.000	51851	11081638
1.870	52773	11073810	3.100	51781	11081638
1.890	52663	11074500	3.200	51711	11081740
1.927	52733	11074010	3.300	51641	11081569
1.947	52723	11074195	3.350	51631	11081569
1.960	52703	11074235	3.400	51621	11081480
1.980	52687	11074525	3.600	51621	11081480
2.000	52660	11075060	3.800	51621	11081480
2.020	52640	11075742			

Table 2. Continued.

Sample No. Nb-OJ-4-86		Run No. 137	T = 8.626 K		
ISOL	M	R	ISOL	M	R
0.000	52821	11072950	1.726	52290	11079400
0.300	52821	11072950	1.730	52292	11079652
0.600	52821	11072950	1.735	52291	11079380
0.900	52821	11072950	1.740	52291	11079492
1.200	52821	11072950	1.750	52281	11079492
1.300	52774	11073270	1.773	52266	11079494
1.400	52634	11074850	1.800	52249	11079732
1.450	52716	11073954	1.852	52219	11079970
1.500	52773	11073464	1.900	52196	11080166
1.551	52763	11073617	2.003	52136	11080369
1.602	52723	11074018	2.100	52089	11080580
1.653	52667	11074837	2.200	52035	11080867
1.670	52645	11075405	2.300	51964	11081142
1.673	52597	11076376	2.400	51900	11081428
1.676	52599	11076540	2.500	51815	11081475
1.679	52605	11076273	2.600	51724	11081448
1.686	52571	11076704	2.651	51690	11081520
1.690	52543	11077463	2.700	51650	11081478
1.696	52494	11078323	2.750	51630	11081370
1.700	52400	11079508	2.800	51613	11081369
1.705	52307	11080240	2.850	51611	11081230
1.710	52237	11080845	2.900	51611	11081230
1.716	52229	11080415	3.050	51611	11081230
1.720	52270	11079838	3.200	51611	11081230

Table 2. Continued.

Sample No. Nb-0J-4-86	Run No. 138	T = 8.712 K
ISOL	M	R
0.000	52815	11072985
0.300	52815	11072985
0.600	52815	11072985
0.900	52815	11072985
1.100	52815	11072985
1.200	52745	11073708
1.300	52600	11075282
1.400	52758	11073460
1.500	52656	11075028
1.512	52638	11075768
1.521	52566	11076730
1.533	52407	11079205
1.543	52200	11081000
1.552	52269	11079482
1.572	52269	11079430
1.582	52269	11079605
1.593	52253	11079431
1.600	52242	11079610
1.700	52182	11079924
1.800	52132	11080340
1.900	52070	11080524
2.000	52010	11080840
2.100	51930	11081288
2.200	51850	11081465
2.300	51743	11081567
2.350	51695	11081440
2.400	51655	11081385
2.450	51634	11081375
2.500	51604	11081280
2.550	51604	11081280
3.000	51604	11081280

Table 2. Continued.

Sample No. Nb-OJ-4-86 ISOL	Run No. 139 M	R	T = 8.797 K
0.000	52816	11072810	
0.300	52816	11072810	
0.600	52816	11072810	
0.900	52816	11072810	
0.960	52800	11073145	
0.983	52773	11073314	
1.003	52762	11073460	
1.023	52725	11073750	
1.043	52686	11074340	
1.063	52620	11074909	
1.080	52630	11074740	
1.100	52710	11073920	
1.120	52761	11073408	
1.141	52771	11073325	
1.161	52770	11073460	
1.180	52743	11073635	
1.200	52713	11074097	
1.220	52659	11074713	
1.240	52619	11075961	
1.260	52439	11078360	
1.270	52180	11080956	
1.281	52270	11079465	
1.291	52263	11079466	
1.360	52204	11079878	
1.400	52174	11080095	
1.500	52104	11080482	
1.600	52024	11080830	
1.700	51944	11081313	
1.800	51834	11081540	
1.850	51774	11081621	
1.900	51717	11081620	
1.950	51667	11081523	
1.970	51647	11081500	
1.930	51637	11081468	
1.990	51637	11081468	
2.000	51629	11081468	
2.200	51610	11081468	
2.100	51610	11081468	
2.050	51610	11081468	
2.030	51615	11081350	
2.020	51623	11081350	

Table 2. Continued.

Sample No. Nb-OJ-4-86	Run No. 140	T = 8.911 K
ISOL	M	R
0.000	52823	11072781
0.600	52823	11072781
0.700	52813	11072991
0.760	52710	11073815
0.790	52650	11074709
0.800	52670	11074201
0.810	52735	11073660
0.825	52777	11073350
0.855	52767	11073411
0.870	52737	11073841
0.890	52627	11075775
0.895	52597	11076405
0.900	52557	11076941
0.905	52447	11078669
0.910	52290	11080690
0.912	52200	11081445
0.914	52180	11081085
0.916	52190	11080750
0.918	52220	11080000
0.920	52242	11079621
0.930	52255	11079550
0.950	52217	11079770
1.000	52157	11080222
1.010	52144	11080222
1.100	52054	11080705
1.200	51934	11081450
1.250	51850	11081682
1.300	51750	11081683
1.350	51684	11081552
1.400	51634	11081442
1.450	51615	11081380
1.500	51615	11081380
1.600	51615	11081380
1.430	51617	11081380
1.420	51621	11081380
1.410	51627	11081380
1.400	51634	11081380

Table 2. Continued.

	Sample No. Nb-OJ-4-86	Run No. 141	T = 9.025 K		
ISOL	M	R	ISOL	M	R
0.000	52814	11072925	0.640	52064	11080870
0.200	52814	11072925	0.660	52027	11081215
0.400	52814	11072925	0.680	51907	11081300
0.470	52744	11073605	0.700	51867	11081530
0.480	52680	11074395	0.720	51867	11081530
0.485	52670	11074444	0.740	51787	11081565
0.490	52675	11074444	0.760	51737	11081565
0.495	52730	11073810	0.780	51692	11081565
0.500	52760	11073415	0.800	51652	11081565
0.505	52770	11073419	0.820	51632	11081390
0.510	52780	11073380	0.840	51623	11081375
0.515	52783	11073380	0.860	51623	11081375
0.520	52773	11073380	0.900	51623	11081375
0.530	52753	11073625	0.830	51628	11081375
0.535	52663	11075435	0.680	51908	11081370
0.540	52613	11076250	0.660	51938	11081162
0.545	52453	11078769	0.640	51991	11080940
0.546	52423	11079130	0.620	52014	11080840
0.548	52340	11080120	0.600	52044	11080708
0.550	52223	11081482	0.580	52084	11080532
0.552	52203	11081220	0.560	52134	11080120
0.554	52210	11080500	0.555	52144	11080231
0.556	52230	11079890	0.550	52114	11081890
0.558	52240	11079575	0.552	52134	11081000
0.560	52260	11079621	0.544	52164	11080000
0.565	52230	11079631	0.550	52110	11081920
0.580	52194	11079920	0.548	52084	11082555
0.590	52173	11080070	0.546	52174	11081730
0.600	52142	11080250	0.680	51958	11081390
0.620	52102	11080500			

Table 2. Continued.

Sample No. Nb-OJ-4-86 Run No. 142 T = 9.037 K

ISOL	M	R
0.000	52820	11072440
0.100	52820	11072440
0.200	52820	11072440
0.300	52820	11072440
0.400	52820	11072440
0.420	52798	11072455
0.436	52763	11072995
0.446	52713	11073675
0.450	52670	11074164
0.457	52681	11073877
0.463	52704	11074930
0.470	52747	11073085
0.480	52779	11072860
0.490	52779	11072860
0.501	52739	11073573
0.506	52619	11076119
0.511	52410	11078800
0.513	52307	11079839
0.515	52238	11080827
0.518	52200	11080756
0.520	52232	11079738
0.522	52239	11079045
0.524	52242	11079205
0.526	52235	11079195
0.530	52222	11079290
0.540	52205	11079544
0.562	52151	11079935
0.580	52107	11080382
0.600	52061	11080429
0.640	51953	11081268
0.680	51826	11081228
0.721	51720	11081140
0.740	51670	11081152
0.750	51651	11081011
0.760	51637	11080937
0.770	51617	11080910
0.781	51617	11080910
0.800	51617	11080910
0.900	51617	11080910

Table 2. Continued.

Sample No. Nb-OJ-4-86 Run No. 143 T = 9.064 K		
ISOL	M	R
0.000	52810	11072450
0.100	52810	11072450
0.200	52810	11072450
0.300	52810	11072450
0.366	52767	11072969
0.375	52716	11073495
0.380	52675	11074030
0.385	52683	11071947
0.390	52710	11073610
0.400	52784	11072832
0.410	52784	11072832
0.421	52756	11073466
0.425	52576	11076735
0.427	52482	11078366
0.429	52362	11079814
0.431	52280	11080540
0.433	52199	11081525
0.434	52201	11081005
0.435	52233	11080095
0.437	52251	11079410
0.440	52243	11079242
0.460	52173	11079750
0.480	52110	11080315
0.523	51982	11081065
0.560	51833	11081282
0.580	51762	11081242
0.590	51730	11081125
0.600	51700	11081120
0.610	51672	11081005
0.621	51654	11080950
0.631	51626	11080950
0.636	51626	11080950
0.646	51626	11080950
0.656	51626	11080950

Table 2. Continued.

Sample No. Nb-0J-4-86	Run No. 144	T = 9.078 K
ISOL	M	R
0.000	52810	11072402
0.100	52810	11072402
0.200	52810	11072402
0.300	52780	11072530
0.338	52690	11073534
0.348	52680	11074065
0.358	52747	11073175
0.370	52777	11072962
0.380	52767	11073135
0.387	52507	11077847
0.388	52387	11079569
0.389	52347	11079889
0.390	52279	11080709
0.391	52259	11081020
0.392	52219	11081512
0.393	52180	11081268
0.394	52189	11081396
0.395	52213	11080485
0.396	52230	11079782
0.397	52240	11079564
0.398	52243	11079479
0.400	52243	11079232
0.403	52213	11079232
0.410	52193	11079630
0.430	52113	11080289
0.450	52043	11080705
0.471	51966	11081170
0.493	51890	11081170
0.510	51810	11081295
0.520	51764	11081194
0.530	51724	11081185
0.540	51700	11081212
0.550	51660	11081103
0.555	51653	11081025
0.560	51653	11080905
0.613	51613	11080915
0.600	51629	11080915
0.590	51629	11080889
0.580	51629	11080889
0.568	51633	11080825
0.560	51635	11080825
0.550	51670	11081052

Table 2. Continued.

Sample No. Nb-OJ-4-86   Run No. 145   T = 9.105 K

ISOL	M	R
0.000	52810	11072768
0.100	52810	11072768
0.200	52810	11072768
0.274	52670	11074492
0.250	52800	11072912
0.255	52790	11072827
0.260	52780	11073060
0.267	52740	11073400
0.272	52690	11074425
0.277	52690	11074332
0.282	52730	11073609
0.287	52777	11073045
0.295	52777	11073200
0.300	52755	11073619
0.305	52475	11079100
0.306	52368	11080435
0.307	52318	11080834
0.308	52298	11081153
0.3098	52210	11082065
0.311	52170	11081970
0.312	52203	11080953
0.313	52205	11080827
0.314	52205	11080029
0.317	52210	11080030
0.320	52202	11079778
0.326	52169	11080106
0.340	52101	11080700
0.361	51988	11081295
0.371	51930	11081495
0.380	51879	11081505
0.390	51834	11081532
0.400	51784	11081460
0.410	51756	11081296
0.420	51706	11081467
0.430	51676	11081415
0.435	51646	11081060
0.440	51646	11081173
0.446	51638	11081135
0.456	51638	11081135
0.480	51638	11081135
0.500	51631	11081110
0.600	51631	11081110

Table 2. Continued.

Sample No. Nb-0J-4-86	Run No. 146	T = 9.133 K
ISOL	M	R
0.012	52824	11072884
0.160	52824	11072884
0.193	52754	11073440
0.198	52700	11074222
0.201	52661	11074752
0.204	52650	11074890
0.207	52714	11073937
0.210	52764	11073534
0.213	52781	11073262
0.216	52781	11073332
0.218	52755	11073630
0.220	52715	11074752
0.222	52529	11078970
0.223	52449	11080078
0.224	52343	11081522
0.225	52253	11082340
0.226	52202	11082905
0.227	52152	11083100
0.228	52145	11082600
0.229	52159	11082455
0.230	52165	11081010
0.231	52166	11080662
0.233	52155	11080600
0.235	52141	11080720
0.243	52081	11080710
0.251	52031	11081090
0.260	51940	11081365
0.270	51870	11081475
0.277	51830	11081552
0.283	51780	11081536
0.289	51746	11081320
0.295	51716	11081313
0.302	51686	11081200
0.307	51656	11081245
0.314	51640	11081120
0.319	51640	11081120
0.333	51640	11081120
0.400	51643	11081224

Table 2. Continued.

Sample No. Nb-0J-4-86	Run No. 147	T = 9.147 K
ISOL	M	R
0.000	52819	11072750
0.130	52819	11072750
0.150	52789	11073038
0.157	52729	11073761
0.162	52669	11074600
0.164	52639	11075505
0.166	52639	11075200
0.168	52662	11074975
0.171	52732	11073960
0.173	52742	11073770
0.175	52772	11073530
0.177	52750	11074080
0.180	52600	11078065
0.182	52420	11080380
0.183	52330	11081625
0.184	52220	11081750
0.184	52270	11082320
0.185	52200	11083345
0.186	52140	11083500
0.187	52120	11083704
0.188	52140	11083195
0.189	52140	11082914
0.190	52110	11081545
0.195	52100	11081100
0.200	52050	11081150
0.210	51950	11081372
0.220	51860	11081492
0.230	51780	11081515
0.235	51740	11081531
0.240	51700	11081458
0.245	51680	11081280
0.250	51660	11081125
0.255	51645	11081118
0.260	51645	11081118
0.270	51645	11081118
0.300	51645	11081118

Table 2. Continued.

	Sample No. Nb-OJ-4-86		Run No. 148	T = 9.158 K	
ISOL	M	R	ISOL	M	R
0.000	52830	11072650	0.156	52077	11081470
0.100	52820	11072805	0.157	52047	11081463
0.122	52800	11073035	0.158	52057	11081240
0.129	52772	11073692	0.161	52035	11081243
0.133	52572	11075455	0.165	51973	11081242
0.135	52572	11076527	0.170	51920	11081500
0.137	52612	11076220	0.175	51860	11081405
0.139	52682	11075235	0.180	51814	11081510
0.141	52704	11074655	0.185	51759	11081287
0.143	52708	11074565	0.187	51749	11081320
0.146	52650	11076560	0.189	51730	11081340
0.1475	52470	11079915	0.191	51716	11081225
0.148	52410	11080675	0.193	51705	11081104
0.1485	52370	11082512	0.195	51700	11081145
0.149	52310	11082100	0.197	51673	11081182
0.1495	52300	11082300	0.199	51673	11081206
0.150	52220	11083791	0.223	51644	11081035
0.1505	52150	11084005	0.217	51644	11081020
0.151	52100	11084350	0.212	51654	11081070
0.1515	52120	11084352	0.206	51662	11081085
0.152	52106	11084445	0.201	51671	11081138
0.1525	52078	11084280	0.196	51685	11081105
0.153	52064	11084085	0.191	51712	11081275
0.1535	52100	11083925	0.186	51752	11081207
0.154	52080	11084070	0.246	51635	11080952
0.1545	52070	11083760	0.260	51632	11081015
0.155	52070	11082550			

Table 2. Continued.

Sample No. Nb-0J-4-86	Run No. 149	T = 9.172 K
ISOL	M	R
0.000	52834	11072403
0.031	52814	11072405
0.050	52816	11072405
0.060	52814	11072405
0.070	52814	11072405
0.080	52813	11072320
0.090	52796	11072690
0.095	52726	11074044
0.096	52680	11074554
0.097	52660	11074802
0.098	52650	11075026
0.099	52650	11075115
0.101	52630	11075700
0.102	52580	11076740
0.103	52521	11077232
0.104	52471	11078803
0.105	52350	11081334
0.106	52260	11082500
0.107	52120	11084115
0.108	52010	11084949
0.109	51930	11085209
0.110	51874	11085030
0.111	51848	11084095
0.112	51849	11083185
0.113	51859	11081996
0.115	51799	11081590
0.117	51869	11081491
0.119	51840	11081200
0.122	51830	11081172
0.161	51630	11080650
0.150	51630	11080650
0.140	51665	11080655
0.130	51737	11080870
0.120	51824	11080838
0.110	51884	11084482
0.180	51630	11080730
0.170	51630	11080730
0.155	51632	11080780
0.149	51640	11080580
0.144	51650	11080658
0.137	51690	11080725

Table 2. Continued.

	Sample No. Nb-OJ-4-86		Run No. 150	T = 9.176 K	
ISOL	M	R	ISOL	M	R
0.011	52870	11071730	0.098	52090	11083272
0.086	52640	11074913	0.099	52070	11082245
0.087	52660	11074915	0.100	52090	11080525
0.088	52670	11074915	0.101	52090	11080585
0.090	52650	11075320	0.102	52070	11080355
0.080	52800	11071910	0.103	52030	11080300
0.081	52790	11072210	0.104	52010	11080395
0.082	52755	11072685	0.105	52000	11080407
0.083	52715	11073062	0.106	52000	11080322
0.084	52705	11073452	0.107	51910	11080415
0.085	52647	11074037	0.108	51907	11080418
0.086	52677	11074363	0.111	51857	11080252
0.087	52650	11074530	0.113	51837	11080389
0.088	52650	11074452	0.115	51790	11080320
0.089	52630	11074868	0.117	51784	11080420
0.090	52710	11074938	0.119	51734	11080246
0.091	52650	11076740	0.121	51723	11080248
0.092	52540	11078135	0.123	51725	11080292
0.093	52450	11080055	0.125	51724	11080162
0.094	52310	11081660	0.127	51706	11080206
0.095	52250	11083025	0.129	51728	11080222
0.096	52160	11083822	0.140	51718	11080500
0.097	52140	11083779			

Table 2. Continued.

Sample No. Nb-0J-4-86	Run No. 151	T = 9.181 K
ISOL	M	R
0.000	52870	11071360
0.022	52860	11071509
0.030	52860	11071509
0.040	52860	11071509
0.050	52860	11071509
0.060	52860	11071509
0.064	52842	11071718
0.066	52822	11072042
0.068	52762	11072163
0.070	52679	11073808
0.072	52624	11075035
0.073	52602	11075452
0.074	52605	11075572
0.075	52595	11076093
0.076	52580	11076568
0.077	52552	11078178
0.078	52522	11079032
0.079	52356	11081132
0.080	52280	11082600
0.081	52121	11083960
0.082	52077	11084088
0.083	52026	11083575
0.084	52000	11082632
0.085	52005	11080460
0.090	51900	11080095
0.096	51790	11080015
0.101	51740	11080192
0.106	51700	11080176
0.111	51696	11079960
0.119	51696	11079900
0.130	51696	11080390

Table 2. Continued.

Sample No. Nb-0J-4-86			Run No. 153	T = 8.974 K	
ISOL	M	R	ISOL	M	R
0.000	52815	11072100	0.729	52243	11079025
0.100	52811	11072154	0.731	52238	11079045
0.200	52811	11071899	0.733	52238	11079018
0.300	52811	11071899	0.735	52238	11078978
0.400	52814	11072385	0.746	52214	11079184
0.456	52822	11072708	0.756	52193	11079416
0.578	52790	11072870	0.777	52157	11079710
0.600	52740	11072988	0.799	52125	11079887
0.615	52680	11073778	0.820	52100	11080098
0.626	52629	11074342	0.841	52070	11080135
0.637	52649	11074219	0.863	52040	11080262
0.648	52732	11072944	0.880	52014	11080574
0.659	52771	11072725	0.900	51987	11080722
0.671	52771	11072600	0.920	51945	11080899
0.682	52771	11072810	0.941	51905	11081038
0.687	52764	11072935	0.961	51859	11081162
0.692	52749	11072900	0.980	51827	11081192
0.697	52728	11073195	1.001	51780	11081090
0.702	52668	11074518	1.020	51734	11081045
0.707	52624	11075617	1.040	51696	11081110
0.712	52554	11076803	1.060	51663	11081005
0.714	52366	11079142	1.080	51626	11080910
0.721	52250	11080269	1.100	51620	11081135
0.723	52157	11080723	1.121	51620	11080900
0.725	52208	11079580	1.151	51620	11080820
0.727	52234	11079290	1.193	51617	11080915